Department of Precision and
Microsystems Engineering

**Inventory of bicycle motion for
the design of a bicycle simulator**

Name: J.H. van den Ouden

Preface

I really enjoyed doing this assignment. The thought that something as common as riding a bicycle is yet far more complicated than one would expect intrigued me. And when I now think of the dynamics of a bicycle the ingenious mechanism still fascinates me.

Also this assignment has learned me a lot more than I would have thought. I gained a lot of respect for scientist who do the same things every day.

First of all I want to thank my supervisors Dr.ir. A.L. Schwab and Ir. J.D.G. Kooijman whom gave me excellent support and were always ready to answer my questions. Their essential input guided me towards todays results.

Special thanks also to my wife Danja who has supported me throughout my education at the technical university. During my graduation she had to sacrifice a lot of time that was otherwise spent together.

Also I would like to thank the other members of the examination committee Prof.dr. D.J. Rixen and Dr.ir. J.L. Herder for their effort that they put into studying the report and the exam.

Furthermore I thank everyone who has helped and provided valuable advise.

Lastly I would like to thank all the test subjects who agreed to ride the measurement bicycle. They voluntary invested their time to do the measurement with no personal interest.

Contents

Chapter 1

Assignment

MSc. Assigment	Bicycle Simulator Design	
Key words	Bicycle, Dynamics, Simulator, Control, Mechatronic Design	
Introduction	The Delft Bicycle Laboratory wishes to develop a bicycle simulator: a stationary bicycle on a moveable platform, driven by a computer model of a bicycle, on which one can sit, steer, lean and pedal. Visual feedback will be done by a single screen with a bicyclist's avatar in a simple Nintendo Wii-like virtual environment.	
Project	For the design of such a bicycle simulator we need to know what the motions are that generally occur during normal bicycling, these are then the motion system requirements for the simulator. Therefore this project should address the following questions: -What are the steer and lean angle, rates and accelerations which occur during normal bicycling? -What are the steer and lean torque exerted by the rider during normal bicycling? Investigate this for three groups of riders: novice (can barely ride a bicycle), average experienced, and elderly riders.	
Project phases	The candidate will start by studying literature on bicycle dynamics and simulators. Next, design an instrumented bicycle to measure the above mentioned quantities. Carry out the measurements on the three different groups. Evaluate the measurements and report the motion system requirements.	

Supervisor Name	Department	Email
Arend L. Schwab	PME/Engineering Dynamics	a.l.schwab@tudelft.nl
Jodi Kooijman	PME/ Engineering Dynamics	jodikooijman@gmail.com

Chapter 2

Introduction

In the Netherlands most people have mastered riding a bicycle. Usually at the age of 4 a child learns to ride a bicycle. Few people however know how a bicycle actually works. A bicycle is a dynamic system that is more complex than one would expect. For example in order to go through a left curve on a bicycle one first has to steer right for a short period of time in order to make the bicycle lean to the left. This effect is called: "counter steering". While going through a left curve one needs to apply torque to the handlebars but not in the direction of the curve. The torque that is applied to the handlebars is to the right and it prevents the handlebars from rotating further. The bicycle as a dynamical system is described in the article "Linearized dynamics equations for the balance and steer of a bicycle: a benchmark and review" [1] written by J. P. Meijaard, Jim M. Papadopoulos, Andy Ruina and A. L. Schwab in 2007.

Many parents worldwide teach their children to ride a bicycle. This is a usually a difficult process because riding a bicycle cannot easily be explained to a child. Training wheels are method to help the child to get used to being on the bicycle.

Figure 2.1: Training wheels offering stability.

However they change the dynamics an the control of a bicycle drastically since the counter steering effect is gone. Losing the trainer wheels is therefore difficult. A regular child picks it up relatively fast however a few trials are inevitable.

For most common vehicles a simulator exists with which a user can learn to control the real vehicle. For example, car simulators, flight simulators, bus simulators, ship simulators etc. For bicycles, a very common vehicle, there is however not even one good simulator available.

Recently a motorcycle simulator was constructed at the university of Padua in Italy. This simulator is described in a paper written by V. Cossalter, R. Lot and S. Rota [6]., A logical next step would be to construct a bicycle simulator. Such a simulator would offer a great advantage to many people who currently have problems with mastering riding a bicycle. For example children with down syndrome don't nearly learn to ride a bicycle as quickly as most children partly because they don't learn at the same rate. Losing the training wheels can be incredibly difficult for them. A bicycle simulator in which adjusting the stability would be as easy a turning a knob with no risk of falling would be a great solution for these children. Adjustable stability is useful because it provides the ability to take smaller steps. With trainer wheels the step of removing the wheels can be too large.

A bicycle simulator also opens up a whole new range of possibilities in physical rehabilitation. After major injuries such as for example losing one arm many people need to master riding a bicycle again. Due to their injuries many people are too afraid of falling and hurting themselves which makes it much more difficult to master riding a bicycle. A bicycle simulator would provide a safe and easy way of regaining their control of the bicycle. Another group that would benefit from a bicycle simulator is those with brain trauma injuries, that have to regain a sense of balance. Current techniques require the patient to walk on a treadmill wearing a harness connected via a rope and the roof to a supervisor, who "catches" the patient incase of a fall, this method often leads to further injuries.

One entirely different thing for which a bicycle simulator could be helpful is for testing virtual prototypes of bicycles. There is no reliable method of calculating the handling qualities of a bicycle model. There are ways to calculate the stability of uncontrolled bicycles, however there is still no proof nor direct indication that the stability of a bicycle is a measure for its handling qualities. Since handling and stability are not the same thing. Using a bicycle simulator research for measurement of handling qualities would be made much easier.

A different party that would be interested is racing cyclists. The best way of training is not always to get on your bike and go outside. For this reason many indoor trainers have been developed. None of these trainers provide a realistic biking experience. The rider never needs to worry about stabilizing

his bike although this is always required during the race. A realistic bicycle simulator would provide the rider with a realistic biking experience in a safe and predefined environment.

In this report the first step in creating a bicycle simulator will be made. The question what are the requirements for a bicycle in terms of for example steer torque, steer angle, lean angle etc. will be answered. This will provide a set of requirements for the actual construction of a bicycle simulator. In order to find the requirements measurements will be conducted using a bicycle equipped with sensors. From these measurements conclusion will be drawn in order to find requirements for a bicycle simulator.

First in chapter 3 an overview is given of simulators that already exist and how a bicycle simulator could work. Next in chapter 4 the parameters that are important for a bicycle simulator are determined and explained in further detail.

Chapter 5 describes the measurements. The different sensors that were installed on the bicycle are discussed and their function is explained in detail. In chapter 6 the desired groups of test subjects are determined and the requirement for the number of test subjects is explained. The final amount of test subjects is also given in this chapter. Next the measurement protocol is described in chapter 7. This protocol is a description of the different things that are registered and the method of starting the measurement.

In chapter 8 the method of filtering the measured data is chosen. Next a part of the data is shown and tests are done in order to get an idea of the reliability of the measured data. Chapter 9 describes the limited range of the sensors and the problems that are caused by that. Next those problems are solved as much as possible and the maximum value is estimated for each of the parameters that were determined in chapter 4.

Finally a conclusion is drawn from this report in chapter 10 and recommendations are given for future research in chapter 11.

Chapter 3

Bicycle simulator

3.1 Available single track simulators

Tacx trainer

Tacx is a company that make bicycle trainers for training indoors. One of their most advanced trainers is the Tacx Fortius Multiplayer trainer. Figure 3.1 shows a picture of this trainer.

The Tacx trainer responds to the following inputs.

- The rotation of the rear wheel
- The steer angle

The outputs of the Tacx trainer.

- The torque from the motor brake that is connected to the rear wheel applies an appropriate resistance simulating things such as: drag, tilt, rolling resistance etc.
- Visual feedback, the rider is riding through a virtual world

As the name of this trainer suggests there is the possibility to do a multiplayer session. A second rider can participate which will then be visible on screen as the rider's opponent.

This system has some drawbacks which make this an unsuitable simulator for learning to ride a bicycle.

- When placed in the simulator the bicycle is held in upright position. There is no lean angle to simulate the rider leaning into the curve. This has as a result that rotating the handlebars to the left means that the bicycle will make a left turn. The counter steering effect is no longer present.

Figure 3.1: The Tacx Fortius Multiplayer trainer meant to simulate the biking experience.

- The lack of a roll angle makes the required steer angle to go though a curve larger than in reality. This is due to the fact that the rider travels a smaller distance when the rider is able to lean into the curve.

- The bicycle on the screen cannot fall over.

As a result it is impossible to learn how to ride a bicycle using this system. This is not surprising since this trainer is meant for experienced cyclists.

Motorcycle simulator

At the Motorcycle dynamics department of the university of Padua in Italy a motorcycle simulator was developed. This simulator is described in a paper [6] called "On the Validation of a Motorcycle Riding Simulator" written by V. Cossalter, R. Lot and S. Rota. Another paper that describes this simulator is the paper [7] called "Objective and subjective evaluation of an advanced motorcycle riding simulator" written by V. Cossalter, R. Lot and S. Rota.

The input of the motorcycle simulator is the following.

- The torque applied to the handlebars which is measured by a torque sensor.

- The force the rider applies to the footrests is measured by load sensors. The difference between left and right is used to calculate the lean torque which the rider applies.

The output of the simulator is the following.

- The lean angle.

- The pitch angle. This can be described as the backward and forward tilt of the simulator. This angle is used to simulate accelerating and braking.

- The yaw angle. This can be described as the "heading" of the simulator. This rotation is limited to 15° in each direction.

- The steer angle.

- The lateral acceleration in order to simulate the centripetal acceleration and lateral acceleration caused by the angular acceleration of a bicycle in the roll direction.

- Visual feedback on three screens surrounding the rider. The simulator provides a first person view so the view rotates with the orientation of the bicycle.

- 3D audio feedback.

Since the yaw angle and the lateral acceleration are limited to a certain range or duration the output of the motorcycle model is filtered using a so called washout filter.

For example say the rider of the simulator starts going around a roundabout. The lateral acceleration that is necessary to simulate the centripetal acceleration cannot be applied constantly since the lateral displacement of the simulator is limited to a certain range. In order to be able to apply an acceleration for a longer time the earth's gravitational field is used. The instantaneous accelerations are still applied by the lateral displacement actuator, however this acceleration will quickly be replaced by earths gravitational field. This means that the the simulator will rotate back a certain angle in the roll direction. On the screen the roll angle is still even larger than in reality.

The simulator located at Padua University is shown in figure 3.2.

3.2   Bicycle model

Virtually simulating the motion of a bicycle is not new, in fact the most famous linearized model of the lateral dynamics of a bicycle was constructed at the end of the nineteenth century by J. W. Whipple. [8] This model was described in the March number of the Quarterly Journal of pure and applied mathematics. It is the same model that is still used nowadays. The same dynamic equations are used in the article "Linearized dynamics equations for the balance and steer of a bicycle: a benchmark and review" [1] written by J. P. Meijaard, Jim M. Papadopoulos, Andy Ruina and A. L. Schwab in 2007.

The input for this bicycle model is the torque applied in the roll direction of the bicycle (T_ϕ) along with the torque applied to the handlebars of the bicycle

(a)

(b)

Figure 3.2: The motorcycle simulator developed by the motorcycle dynamics department at Padua University in Italy.
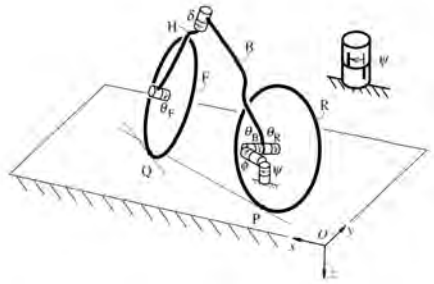
Figure 3.3: The bicycle in the model shown in the coordinate system that is used.

(T_δ). The output of the model is the lean angle of the bicycle (ϕ) and the steer angle of the handlebars relative to the bicycle (δ).

The linearized differential equation that governs the motion of the bicycle.

$$M\ddot{q} + vC_1\dot{q} + [gK_0 + v^2 K_2]q = f \qquad (3.1)$$

In which $q = [\ \phi \quad \delta \ ]^T$ and $f = [\ T_\phi \quad T_\delta \ ]^T$.

When ϕ, δ and v are known, other things such as the heading and the position of the bicycle can be found.

The heading of the bicycle can be found using the following relation.

$$\dot{\psi} = \frac{\delta v + \dot{\delta}c}{w} \cos\lambda \qquad (3.2)$$

In which v represents the forward speed of the bicycle, c represents the trail of the bicycle and w is the wheel base of the bicycle. Time integration of this $\dot{\psi}$ gives the heading ψ.

The horizontal velocity in x and y direction, assuming the bicycle starts in x direction is then given by.

$$\begin{aligned} \dot{x} &= v \cdot \cos\psi \\ \dot{y} &= -v \cdot \sin\psi \end{aligned} \qquad (3.3)$$

Integrating these quantities over time gives x and y.

Although this linearized model is from the nineteenth century this model is the most frequently used model by scientists active in the field of bicycle dynamics.

Figure 3.4: The three rotations of a bicycle.

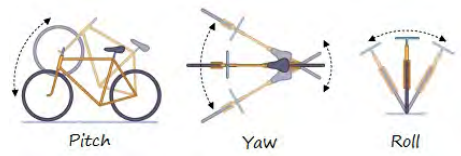## 3.3 Bicycle motion

A rider controls a bicycle by doing the following things. These things are referred to as the inputs of the bicycle.

- Exert torque in order to rotate the handlebars.

- Move his center of mass in lateral direction which imposes a torque in the roll direction.

- Apply a torque to the pedals in order to accelerate the bicycle.

- Brake in order to decelerate the bicycle.

The bicycle moves and rotates in different directions. For convenience the rotations are named: pitch, yaw and roll. The different rotations associated with these names ar shown in figure 3.4.

These rotations and movements are experienced by the rider on the bicycle. In order to investigate what a simulator should be able to do first a summary will be given of the main parameters that a rider can notice. This is referred to as the outputs of the bicycle.

- The bicycle can rotate in the pitch direction.

- The bicycle can rotate in the yaw direction.

- The bicycle can rotate in the roll direction.

- The bicycle can accelerate in forward direction. The bicycle can decelerate as well while braking, the rate of this deceleration is dependent on the quality of the brakes.

- The bicycle can accelerate the rider laterally; For example during cornering.

- The bicycle can impose a torque on the handlebars, this is caused by a combination of gyroscopic effect and gravity acting on the steering assembly.

The way these outputs of the bicycle respond to the inputs is governed by the bicycle's dynamics. This is described by the bicycle model discussed in section 3.2.

3.4 Simulation

Mechanical

Ultimately what the bicycle simulator should be able to do in order to simulate the complete bicycling experience is the following.

- Measure the torque in the roll direction.

- Measure the force that is applied to the pedals. Alternatively the pedals can be connected to a motor brake providing the proper resistance, the speed of the pedals can then be measured. This in an input for the model.

- Measure the torque that is applied to the handlebars about its axis of rotation, this is also an input for the model.

- Rotate the rider about the longitudinal axis which is the axis trough both of the contact points of the tires with the ground (roll).

- Rotate the rider about the vertical axis which is a vertical axis trough the contact point of the rear tire (yaw).

- Rotate the rider about the lateral axis which is a horizontal axis orthogonal to the longitudinal axis through the contact point of the rear tire (pitch).

- Rotate the handlebars

- Displace the entire assembly in lateral direction in order to simulate the centripetal force when going through curves.

- Apply an acceleration in forward direction. Alternatively this can be done by tilting the rider in forward and backward direction.

In order to give the rider a realistic bicycling experience the rotations and consequently the angular velocities, angular accelerations, angular jerk etc. should be the same as on a real bicycle. If this is not possible, the simulator should give the rider the impression he is riding an actual bicycle.

Multimedia feedback

An intuitive visual interface is very important for a bicycle simulator. The rider should be able to see his orientation, heading and his speed easily.

Later more software features can be included after the construction of a working simulator. For example a virtual graphical surrounding could be created including traffic and traffic lights in order to make the simulator more realistic. An example of the graphical interface of a motorcycle simulator created by Honda is shown in figure 3.5.

Also the rider should have a good impression of his forward speed. For car

Figure 3.5: The interface of a motorcycle simulator created by Honda.

simulators this challenge has proven to be more difficult than just showing it on the screen. The first step is to make the screen as large as possible in the visual field of the rider. Audio feedback is also important to give the rider an idea of how fast he is going. The sound of the rolling tires, the wind and the chain should change in volume and frequency with the forward velocity.

Chapter 4

Design requirements

In order to simulate normal bicycling and make it feel as realistic as possible the simulator should be able to apply the same forces to the rider as the forces that are applied to the rider while he is riding a bicycle. In order to construct a bicycle simulator the forces (or the accelerations) that the simulator should be able to deliver needs to be known beforehand. In this chapter the parameters that are important for the bicycling experience that can be measured are determined.

4.1 Bicycling parameters

Before starting the design of the bicycle simulator the determination of some parameters of normal cycling are of great importance. In this section the parameters related to regular cycling will be considered.

- The forward speed, and acceleration range of the bicycle.

- The angle, the angular velocity, the angular acceleration and the angular jerk range of the roll motion of the bicycle.

- The angular velocity and the angular acceleration range of the yaw motion of the bicycle.

- The steering angle and the angular velocity range of the handlebars.

- The steering torque range applied to the handlebars by the rider.

- The centripetal acceleration range of the rider.

In this list the pitch motion of the bicycle is not mentioned. This is because for learning to ride a bicycle the best would be to start with a level surface. The maximum pitch angle is also relatively small compared with for example the maximum roll angle. This can be seen in the figures displayed in section 8.2. In order to set a realistic objective the pitch motion is left outside of the scope of

this report.

One thing that is also not mentioned in the above list is the force the rider applies to the pedals. This is not required since simulators that are able to simulate the forward motion of a bicycle already exist. Namely the trainers that were developed by Tacx, discussed in section 3.1 of this report. When a bicycle simulator would be developed in cooperation with Tacx, the working principle of the Tacx trainers could be implemented into the bicycle simulator.

4.2   Mechanical parameters

Next a trade off has to be made for which motion to compromise. Which motion is important and which is less important? Also which motions can easily be simulated and which motions are more difficult to replicate? Which motions are important and which are less important is still under debate. There was no useful scientific evidence for which motion to consider important for learning to ride a bicycle and which motion is of less importance. This section suggests an idea which is what is suspected to be sufficient for learning to ride a bicycle.

Yaw angle
First of all the yaw motion is important, however having the correct yaw angle at all times is not as important as having the correct roll angle for example. It is possible for example for riding in a circle to make the ride feel the instantaneous angular velocity and the instantaneous angular acceleration however make the yaw angle return to zero automatically by slow movements. This is possible by applying filters. This way the yaw angle can be limited to for example 15°. This makes the construction of the bicycle simulator easier.

Centripetal acceleration
In order to replicate the feeling of centripetal acceleration that the rider experiences it is possible to accelerate the simulator in lateral direction. A problem however is that when the rider is in steady state cornering the simulator would have to accelerate over an infinite length in lateral direction. In order to overcome this problem again a filter can be applied which limits the lateral position to a certain range. A way of applying the acceleration for a longer period of is by also making use of the earth's gravitational field. The longer a curve takes the more the simulator could reduce it's roll angle. The visual roll angle on the screen could also be important, an exaggerated roll angle on the screen could make the rider experience the curve as more realistic.

Pedalling motion
A torque sensor could be used in order to measure the force the rider applies to the pedals. However a sufficient solution would be a way similar to the way the forward accelerating and decelerating is simulated by the Tacx trainer described in section 3.1. A motor brake could be applied directly to the sprocket connected to the crankshaft of the pedals. The torque applied by the motor brake should then correspond with the friction in the model.

Roll angle, steer angle and steer torque
The roll angle, angular velocity, angular acceleration, steer angle, angular velocity, angular acceleration and the steer torque can be applied by the simulator without any problems. These parameters are without a doubt essential and they should be simulated in a realistic manner.

Chapter 5

Measurement Instrumentation

In order to determine the required range for the bicycling parameters discussed in section 4.1 these quantities needed to be measured. This data was collected using a fully instrumented bicycle. Test subjects were be asked to ride a route through Delft on this bicycle. From this, the range for the parameters discussed in section 4.1 were found.

Figure 5.1 shows the measurement bicycle including a rider and backpack containing a video recorder and a laptop. The bicycle that was used was a "Batavus Browser". Properties of this bicycle are found in a paper [2] named "A method for estimating physical properties of a combined bicycle and rider" written by J. K. Moore, M. Hubbard, J. D. G. Kooijman and A. L. Schwab.

There were three different groups of test subjects. More on these groups and the size of these groups is discussed in section 6.

The measurement bicycle was equipped with a MTI-g orientation sensor which is connected to a notebook via USB. Furthermore there are 7 sensors and 2 batteries that are connected to a data acquisition device. Also the rider of the bicycle wears a helmet with a bullet camera installed on it. This helps the analysis of the data since the video shows what the rider is looking at data can be coupled to events. A digital video recorder was used in order to record the video on a memory card. In figure 5.2 is shown how all these sensors were connected.
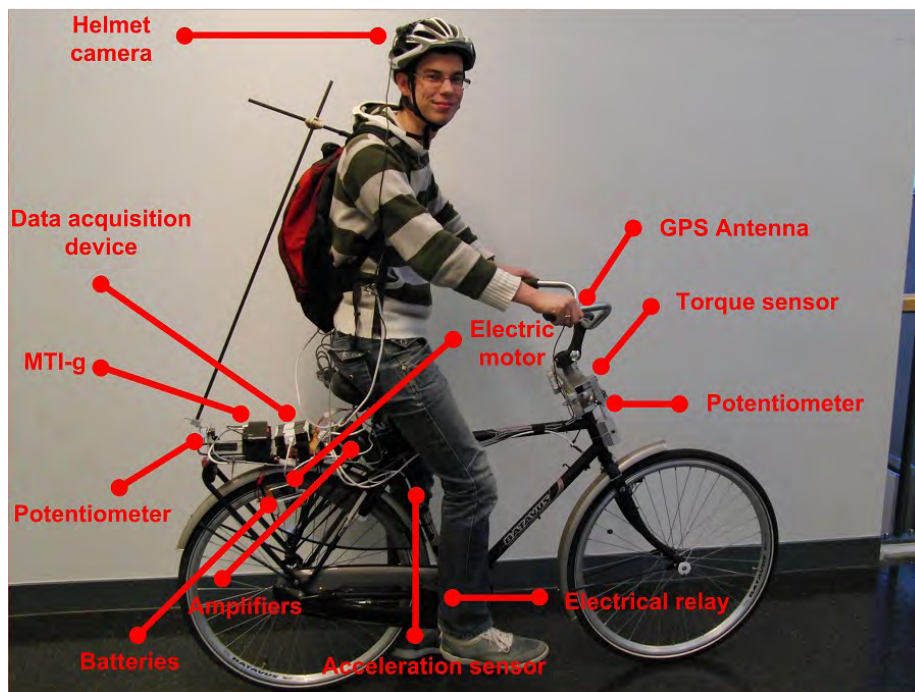
Figure 5.1: The measurement bicycle including rider and backpack containing a video recorder and a laptop. The different components of the measurement bicycle are indicated in the figure.
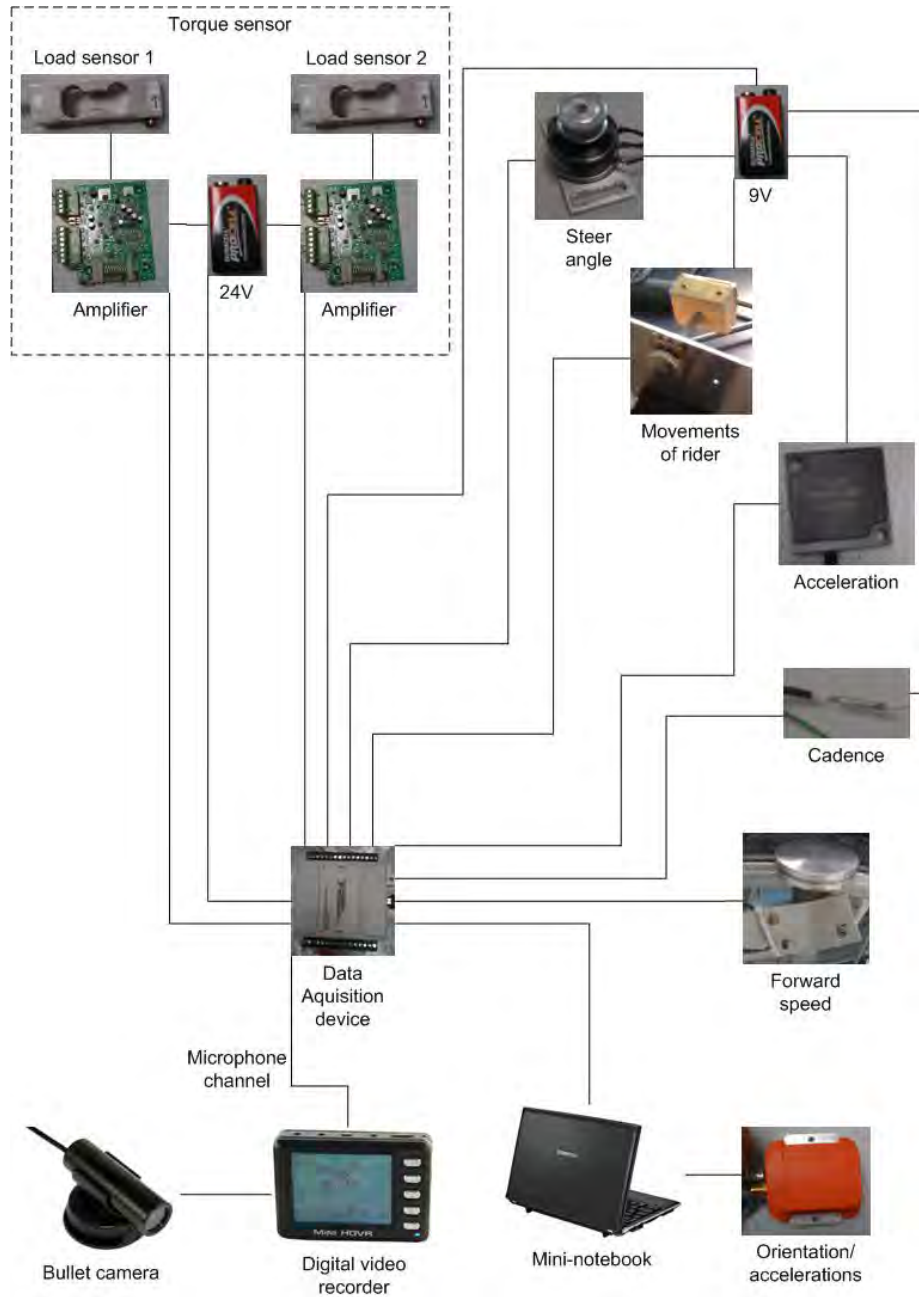
Figure 5.2: The different sensors that were connected to the data acquisition device and the notebook

Device	Brand	Type	Measuring	Specifications
Orientation sensor	Xsens	MTI-g	Orientation, Rotation speed, Acceleration, Position (GPS),	For details about specifications please visit www.xsens.com
Data acquisition device	National Instruments	NI USB-6211	Measuring voltage from 7 sensors	16 analog inputs (16-bit, 250 kS/s) 2 analog outputs (16-bit, 250 kS/s)
Potentiometer	Sakae	CP22E	Rider lean relative to the bicycle	Wirewound, single turn, $10K\Omega\pm$ 3% Linearity $\pm0.5\%$ K8 Electrical travel $355° \pm 5°$
Potentiometer	Feteris	FCP40A	Steer angle	Conductive plastic, 3 turn, Electrical travel $1075° \pm 5°$ $10K\Omega$ Linearity $\pm$ 0.5%
Load sensor (2x)	HBM	HBM PW4MC3	Steer torque	bending beam load sensor, maximum load 30 N, Excitation 5Vdc, Off center load compensated
Amplifier (2x)	Scaime	CPJ-cpj2s	Steer torque signal amplification	Board version, Input 24V $\pm$4V
Electric motor	Maxon	2326.940-12.111-050	Forward velocity	Nominal voltage 18V, maximum speed 5300 rpm, motor constant 32.1 mNm / A, internal resistance 21 Ω
Accelerometer	Feteris	400A	Acceleration for synchronization purposes	Maximum: 20 G, Excitation 12Vdc, Sensitivity 981.5 mV/g
Digital video recorder	Dogcam	Mini HDVR LS H720 v2.0	Video recording on SD card	Resolution D1 PAL 720 x 576 (25fps)
Bullet camera	Dogcam	N.a.	Video	included in DVR package

Table 5.1:
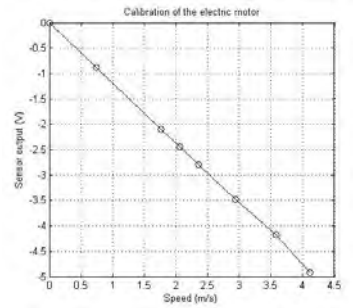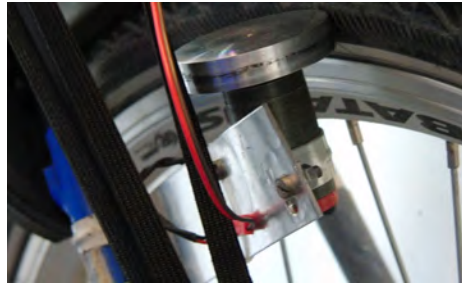
(a) The electric motor that was used in order to measure the forward speed of the bicycle.

(b) The calibration results of the electric motor.

Figure 5.3:

5.1 Forward speed

Apparatus

The forward speed of the bicycle is commonly defined in models as the speed of the contact point between the ground and the rear wheel. The forward speed was therefore measured by measuring the rotation speed of the rear wheel. The rotation speed was measured by an electric motor. The sensor is shown in figure 5.3(a)

Device	Brand	Type	Measuring	Specifications
Electric motor	Maxon	2326.940-12.111-050	Forward velocity	Nominal voltage 18V, maximum speed 5300 rpm, motor constant 32.1 mNm / A, internal resistance 21 Ω

Calibration

Calibration of the electric motor was done using a treadmill. The bicycle was placed on the treadmill and several speeds were measured. The speed of the treadmill was measured using three different measurement systems.

- A display on the treadmill showed the speed at which it was running.

- A digital speed-o-meter installed on the bicycle measured the distance the bicycle had traveled in an amount of time measured using a stopwatch.
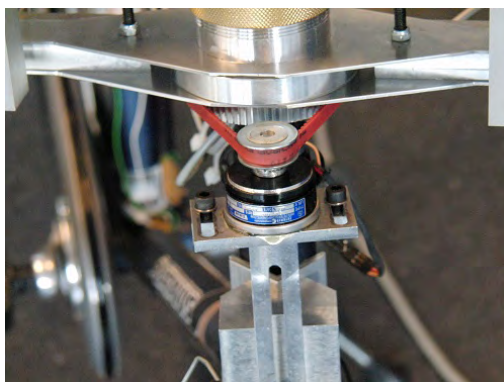
Figure 5.4: The potentiometer connected to the steering assembly.

- A stopwatch and a mark on the band. Counting the number of times the mark passed together with the time that passes and the circumference of the band gives the speed.

The difference in the measured speed from all these measurement systems turned out to be negligible.

The motor output was then measured at the various speeds. The result is shown in figure 5.3(b).

5.2 Steer angle

Apparatus

The steering angle was measured using a potentiometer. The potentiometer that was used is a linear multi turn potentiometer with a conductive plastic resistance. The rotation of the potentiometer is unlimited, this means that when the maximum resistance is reached and the potentiometer is rotated further, the dead band is reached. Rotating 2 degrees further the resistance will change to 0 and start over. The potentiometer was connected to the steering assembly by a toothed belt. The transfer ratio is such that a 90° rotation of the steering assembly (−45° to 45°) equals 3 rotations from the potentiometer, which is the full range of the potentiometer. The configuration is shown in figure 5.4.

(a) The potentiometer which is used in order to measure the body movement of the rider, the arm that is also connected to the backpack is also shown.

(b) The arm connected to the backpack. The arm is connected to the backpack as rigidly as possible using iron wire. Figure 5.1 shows an overview of this system.

Figure 5.5:

Device	Brand	Type	Measuring	Specifications
Potentiometer	Feteris	FCP40A	Steer angle	Conductive plastic, 3 turn, Electrical travel 1075° ± 5° 10KΩ Linearity ± 0.5%

Calibration

Calibration of the potentiometer was done with the bicycle placed in a standard from a Tacx trainer. This standard places the bicycle in upright position, this was checked with a spirit level. Next -45°, 0° and 45° marks were made on the ground. The steering assembly was aligned to each of these marks and the voltage was measured. Since the voltage output of the potentiometer varies linearly with the angle, the corresponding angle can now be found for each voltage using linear interpolation. The voltage of the battery was also measured so that the ratio between the voltage from the potentiometer and the voltage from the battery can be used.

5.3 Body movement

Apparatus

The displacement of the rider's center of mass is required to be able to apply inverse dynamics on the measured data. The rider can either lean into curves, not lean at all or lean out of curves. Also on straight parts the rider moves relative to the bike because the entire body moves due to pedalling motion.

The body movement of the rider was measured using a potentiometer fixed to the luggage carrier of the bicycle. A carbon fibre reinforced tube is attached to the potentiometer in such a way that it measures the sideways movements of the rider on the bicycle. Two hinges allow the rider to move forward and backward. The forward and backward motion is not measured. The potentiometer that was used is a linear multi turn potentiometer with a conductive plastic resistance. The rotation of the potentiometer is unlimited, this means that when the maximum resistance is reached and the potentiometer is rotated further the resistance will change to 0 and start over.The potentiometer is shown in figure 5.5(a), the backpack with the arm connected to it is shown in figure 5.5(b). An overview in which the entire system can be seen in shown in figure 5.1. Note that there are two hinges, one near the potentiometer and one near the backpack. These hinges allow the rider to move forward and backward.

Device	Brand	Type	Measuring	Specifications
Potentiometer	Sakae	CP22E	Rider lean relative to the bicycle	Wirewound, single turn, $10K\Omega\pm$ 3% Linearity $\pm0.5\%$ K8 Electrical travel $355° \pm 5°$

Calibration

The potentiometer was calibrated in a way similar to the potentiometer in section 5.2. The voltage from the potentiometer was measured with the tube being horizontal in both directions and the tube being vertical. Then for every voltage a corresponding angle can be found using linear interpolation. The voltage of the battery was also measured so that the ratio between the voltage from the potentiometer and the voltage from the battery can be used.

From the angle the movement of the rider can be approximated. This is not precise because the stick is connected to the backpack and not to center of mass of the rider, this means that the location of the center of mass of the rider is never exactly known. However the location of the center of mass can be approximated. How this is done is explained in detail in section 8.6.
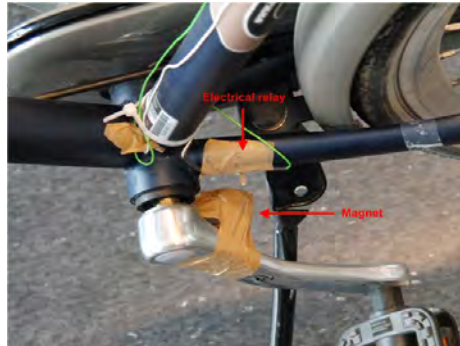
Figure 5.6: The electrical relay used in order to measure the pedalling frequency

5.4 Cadence

The pedalling frequency is measured using an electrical relay. The relay is switched on and off by a magnet which is connected to the crank arm. With each period in the pedalling motion the crank arm passes the relay once. At that instant the switch in the relay is closed and the voltage from the power source connected to it is measured at the output. The configuration is shown in figure 5.6.

5.5 Helmet camera

When analyzing the measurement results it can be useful to known what exactly happened at certain time instants. The rider responds to many disturbances from the outside. For example a rapidly approaching cyclist from the right could make the rider use his brakes and so on. This is why a helmet camera was also incorporated into the measurement instrumentation. This makes it easier to discover what happened at each time instant and also what the rider is looking at.

The video signal from the helmet camera was recorded by a digital video recorder which was put into the backpack that the rider carries. The video was synchronized with the measured data. The method of synchronization is explained in further detail in section 5.8.

Figure 5.7: The Xsens MTI-g orientation sensor on the location where it was connected to the measurement bicycle. The sensor was fixed rigidly to bicycle frame using duct tape with the foam material from the picture between the frame and the sensor. The purpose of the foam material is to provide some damping for the vibrations caused by the road's surface.

Digital video recorder	Dogcam	Mini HDVR LS H720 v2.0	Video recording on SD card	Resolution D1 PAL 720 x 576 (25fps)
Bullet camera	Dogcam	N.a.	Video	included in DVR package

5.6 Orientation sensor

Apparatus

In order to be able to measure the orientation of the bicycle an Xsens MTI-g sensor was used. This sensor gathers the following information:

- The rotation speed of the sensor measured by a 3D gyro sensor.

- Accelerations of the sensor measured by a 3D acceleration sensor.

- The direction of the earth's magnetic field measured by a 3D magnetometer.

- The position of the sensor using a Global Positioning System (GPS).

- The altitude of the sensor using a pressure sensor.

This data is used in order to calculate the orientation of the sensor. A kalman filter is used to process the data in order to find the orientation of the sensor.

The GPS signal for example is compared to the data from the acceleration sensor. This way rotations can be detected. Also the assumption is made that over a period of time the gravity force should always be in the same direction. This is then compared to the signal from the gyro sensor. Data from the magnetometers is also compared to the calculated orientation. The measured pressure is also used in order to calculated the altitude of the sensor. This is then again compared to the GPS data. This way the orientation is calculated as accurately as possible

The MTI-g sensor is connected to the bicycle as shown in figure 5.7. The output data from the sensor is:

- Euler angles

- Position

- Accelerations

- State of the sensor (GPS fix or not)

This data is sent from the sensor to the notebook and recorder by Matlab at a frequency of 50 Hz.

Solving problems

Heading

One problem that occurred during the preparations for the measurements is that the heading was not measured accurately. While stationary the output orientation of the sensor was rotating. This was caused by the integration drift from integrating the rate of turn signal from the gyro sensor. This problem was solved by putting the sensor in a aerospace scenario mode in which the magnetometers are also used. This way the calculated heading is compared to the direction of the earths magnetic field.

GPS

A different problem involved the MTI-g not measuring the orientation correctly and producing incorrect measurement results with at pitch angle of 10 degrees and a roll angle of approximately 10 degrees which both should have been near zero. The cause of this problem was that the sensor did not have a proper GPS fix. Having a GPS fix is important in order to get correct measurement results. This due to the fact that the sensor differentiates the position data from the GPS twice in order to find the accelerations in the global coordinate system. Comparing this with the acceleration in the local coordinate system of the sensor can be used to find the orientation of the sensor.

Calibration

In order to known the orientation of the bicycle, the orientation of the MTI-g sensor in the reference frame of the bicycle must be known. In order to find out this orientation the bicycle was placed in a Tacx trainer standard so that the bicycle would be completely vertical. A spirit level was used to check if the bicycle was vertical. Next the orientation output of the MTI-g sensor was observed after 30 minutes which is more than enough time for the filter of the sensor to stabilize. The offset in the roll and pitch angles caused by misalignment of the MTI-g sensor turned out to be no more than 1.5 degrees.

5.7 Torque sensor

One thing that is suspected to be of importance for a realistic feeling of the simulator is the steer torque. For the purpose of measuring the steer torque accurately a torque sensor was developed. In this section the development of the torque sensor is described.

Pre-estimation of the required range

First of all literature research was done in order to find a required range for this torque sensor.

- A paper [9] written by Kok Y. Cheng, David Bothman and Karl J. Åström, named "Bicycle Torque Sensor Experiment" describes an experiment with a torque wrench connected to the steering assembly. They recorded the maximum torque doing various maneuvers. A maximum steer torque was recorded at a speed of 4.44 m/s of 39.1 cm-kg which is 3.84 Nm.

- Researcher Jason Moore described an experiment with an accurate torque wrench on his web site. The torque wrench was connected to the steering assembly. The maximum of the applied torque while doing several manoeuvres was recorded. The maximum torque that was measured while doing these maneuvers was 4.8 Nm http://biosport.ucdavis.edu/research-projects/bicycle/instrumented-bicycle/steer-torque-measurement

For the purpose of having some more support for the required range of the torque sensor an experiment was done using only a bicycle and two spring scales. The spring scales were connected to the hand grips from the bicycle's handlebars. A test subject rode a number of test courses with the instructions to hold the spring scales and try to look at the maximum value of both the spring scales. Figure 5.8 shows two pictures from this experiment.

The outcome of this experiment was that the required force for one arm to go through curves was no more than 10 N. Since the grips of the handlebar are 0.56 m apart the torque is found in the following way.

$$T = F \cdot l = 10 \cdot 0.28 = 2.8 Nm$$

In this calculation the assumption is made that the force that was applied in the optimal direction around the axis of rotation of the steering assembly. Based on all these indications of what the maximum torque that is applied during normal cycling, the range for the torque sensor was chosen to be at least [-5 Nm, 5 Nm].

Design specifications

First of all the required range for this torque sensor was important.

- The chosen minimum range for the torque sensor is [-5 Nm, 5 Nm].

Figure 5.8: The experiment using spring scales on a bicycle that was done at the parking lot of the 3mE faculty of the TU Delft

- The torque sensor should measure the torque that is used to turn the front wheel within an accuracy range of -15% to + 15%.

- The torque sensor should still measure the torque accurately within these bounds when a force of 40 N is exerted in the downward direction on the handle bar on one side.

Design

The electronic hardware that was used for the torque sensor is shown below.

Device	Brand	Type	Measuring	Specifications
Load sensor (2x)	Feteris	unknown	Steer torque	bending beam load sensor, maximum load 30 N, Excitation 5Vdc
Amplifier (2x)	Scaime	CPJ-cpj2s	Steer torque signal amplification	Board version, Input 24V ±4V

The design of the torque sensor is shown in figure 5.9.

In order to be able to measure only the torque that makes the wheel turn, the first step was to create a structure in which the handlebars would be able to rotate freely independent of the front wheel. Figure 5.10(a) shows this construction. This construction in made making use of angular contact bearings. Figure 5.10(b) shows a cross section of a part of the design in which the bearings are visible.

Now in order to be able to measure the torque, the rotation of the upper part with respect to the lower part is prevented by connecting these parts using a load sensor. This load sensor can withstand a load of maximum 30 N. In order protect the load sensor from overloading an overload protection was added which is adjustable using a setscrew. An overview of the complete design in which the rotation is not free is shown in figure 5.9.

The distance from the load sensors to the central axis of the system is 0.125 m, the torque that the torque sensor can withstand is found in the following way.

$$T = 2 \cdot F_{loadsensor} \cdot l = 2 \cdot 30 \cdot 0.125 = 7.5 Nm$$

Since this is more than the required 5 Nm the load sensor now meets the requirements.
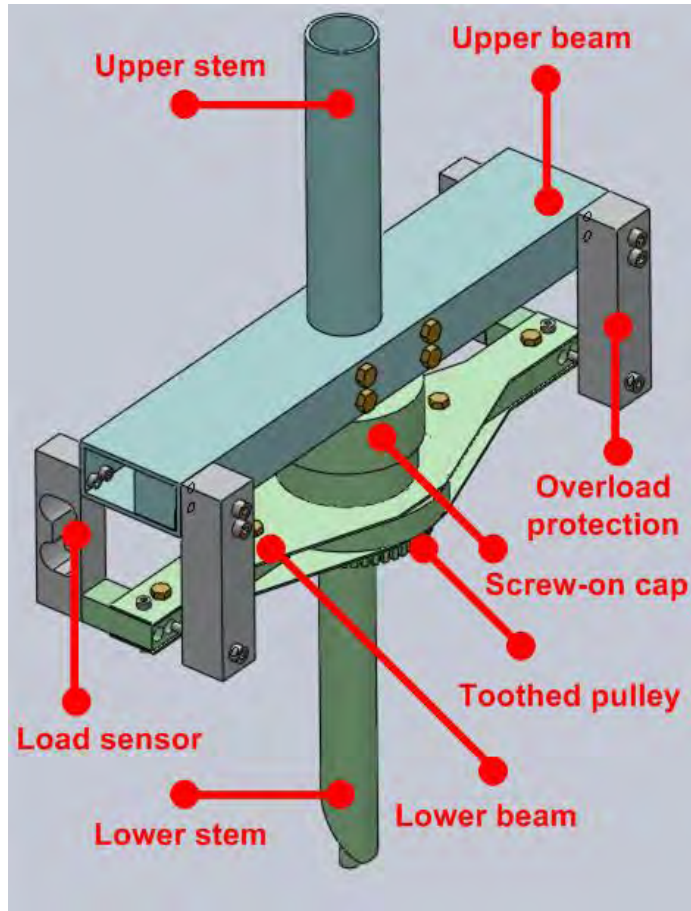
Figure 5.9: The complete design. A short description of the working principle follows. The lower stem can be inserted into the head tube of a bicycle. The handlebars can be connected to the upper stem using a flight feather. Below the screw-on cap two radial contact bearings are located that allow the blue (upper) part to rotate with respect to the green (lower) part. This rotation however is then prevented by the load sensors that are placed between the upper beam and the lower beam. The torque that is transferred from the upper stem to the lower stem is transferred by the two load sensors. The overload protection prevents the load sensor from bending beyond its specified measurement range.
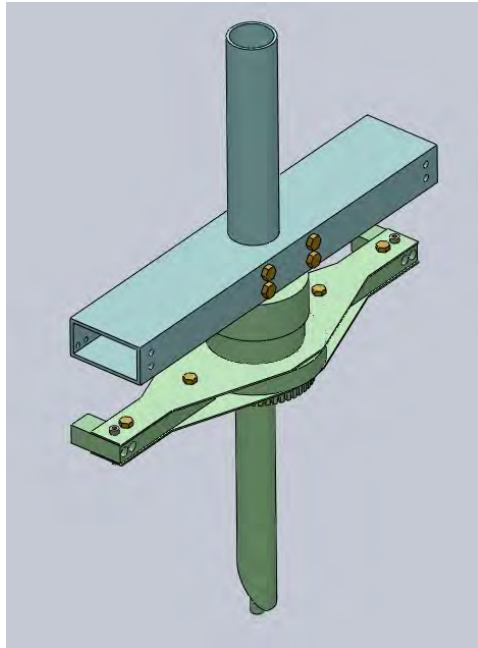
(a) In this construction the handlebars can rotate independent of the steering wheel. The parts that are shown in blue are able to rotate relative to the parts shown in green.
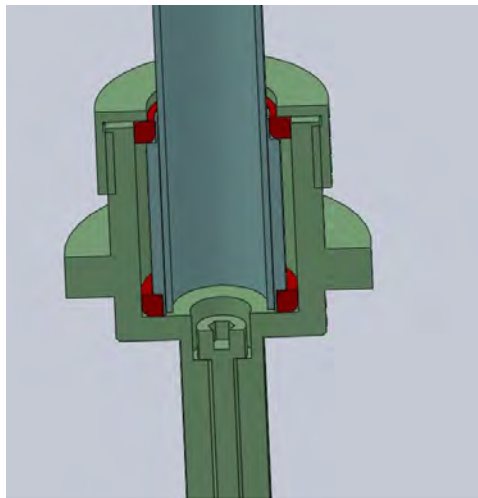
(b) Part of the design, shown in a cross section. The parts that are shown in blue are able to rotate relative to the parts shown in green. The radial bearings that connect the blue and the green parts are shown in the color red. The rotating upper shaft is connected via bearings (red) to the lower shaft that is bolted (bottom) to the front fork. The bearing housing is kept in place by a large screw on cap.

33

Figure 5.10:

Alterations

After the production of the torque sensor a problem was brought to light; the torque was accurately measured by the torque sensor however an axial force exerted on the handlebars had a significant effect on the measured voltage in the load sensors. Several alterations were made to the construction in order to reduce this effect. These alterations are discussed below.

Remove the upper bolts

The bolts that connected the load sensors to the upper beam were removed in order to change the construction from a statically undetermined construction to a statically determined construction. Figure 5.11(b) shows the load sensor in this setup. This change reduced the maximum torque that the sensor was able to withstand from 7.5 Nm to 3.75 Nm. This effect is unwanted however this change was required in order to fix the design of the torque sensor.

Reduce friction

Now that the upper bolts were removed the construction gained a new degree of freedom. When the handlebars were loaded in the downward direction on one side, for example the left side, the entire construction would bend to the left. The result is that the left tip of the upper beam gets closer to the left tip of the lower beam. The load sensors and the overload protection will therefore slide over the surface of the beams. This effect introduces some friction in vertical direction.

In order to reduce this effect the setscrew used in the overload protection was replaced by a setscrew with a rounded tip. Also, because the surface of the lower beam was more smooth than the surface of the upper beam the load sensor was now connection on the upper side and the bolts were removed on the lower side.

Both the surfaces from the overload protection and the load sensor were lubricated with vaseline in an effort to reduce the friction even further.

Pre-stress

One problem of the initial version of the torque sensor was that there was a small clearance between the lower beam and the load sensor. Because riding the bicycle on bumpy roads would exert vibrations in all directions this clearance is unwanted. Impact from the lower beam unto the sensors is not should be prevented since the purpose of the torque sensor is to measure only the steer torque and not some disturbance caused by vibrations. In order to solve this problem a prestress was introduced. This prestress is mean to press the load sensors unto the lower beam so that they keep contact even while vibrating.

(a) The torque sensor in a test configuration without the upper beam.

(b) The torque sensor without the upper bolts of the load sensors.

Figure 5.11:

A setscrew is used in order make this prestress adjustable. A problem with this adjustment was that the overload protection was located exactly where this setscrew would be. To solve this, the overload protections were moved. They were moved 15 mm away from the tips of the beam further towards the center of the construction. The tip of the setscrew is rounded so that the load sensor has a known point of contact and it also reduces friction caused by sharp edges. Figure 5.12(a) shows this setup of the torque sensor.

Remove overload protection

After doing some measurements it turned out that the calibration values were wrong every time. The overload protection seemed to be the problem causing unreliable results. This inconsistency was too difficult to work with. The measure that was taken in order to correct this problem was to remove the overload protection. Of course the load sensors would be overloaded, however they would be overloaded for very short periods of time during the peak loads which are usually of a duration of 100 ms or less. This measure turned out to make the use of the torque sensor much more easy. Figure 5.13(a) shows the calibration of the sensor, which was done twice along with a calibration check that was carried out after the measurements.
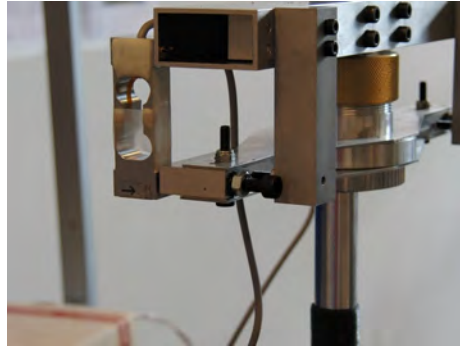
Calibration

The calibration of the torque sensor was done using a pulley and some weights. The handlebars were replaced by a straight tube with stripes on it indicating the length of the lever.

This way a known torque was exerted on the load sensor. Because the upper bolts were removed from the load sensors the exerted torque is transferred into only one of the load sensors. In order to find the relation between torque and the voltage from the sensor various torques were applied to the torque sensor using the weights under various conditions.

Figure 5.13(b) shows an example of the relation between the torque and the output voltage from the sensor. The bounds, that are set by the criteria that the sensor should be 15% accurate with respect to the maximum torque, are also shown in the figure 5.13(b).

An axial force exerted on the handlebars is simulated by connecting weights to the handlebar directly. The effect of this disturbance was investigated. A picture of the calibration setup is shown in figure 5.12(b).

(a) The adjustable pre-tension system, the large bolt is the setscrew that adjusts the pre-tension. Behind it is the overload protection that was moved in order to have the adjustable pre-tension.
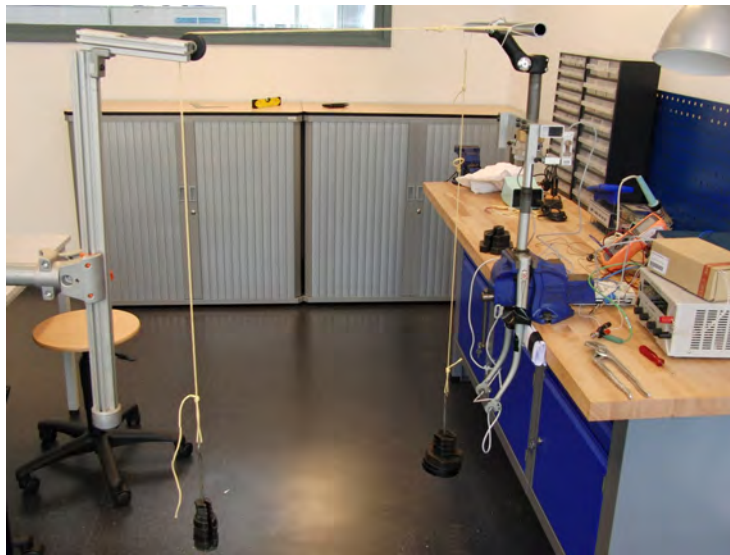
(b) The calibration setup of the torque sensor. The weight on the right is the disturbance load, a purely vertical force imposing a shear force and torque in two directions. The weight on the left is a purely horizontal force imposing a known torque. The orange multimeter on the right shows the voltage output.

Figure 5.12:
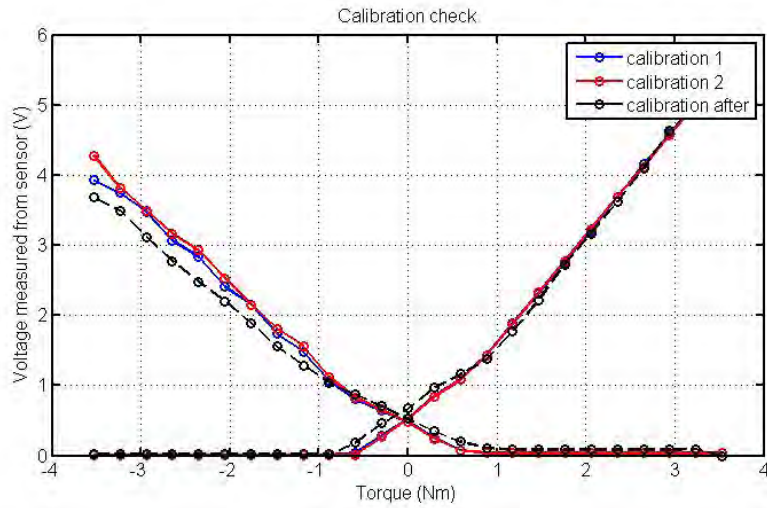
(a) The calibration results showing several calibration sets, the last calibration set is done after doing all the measurements.
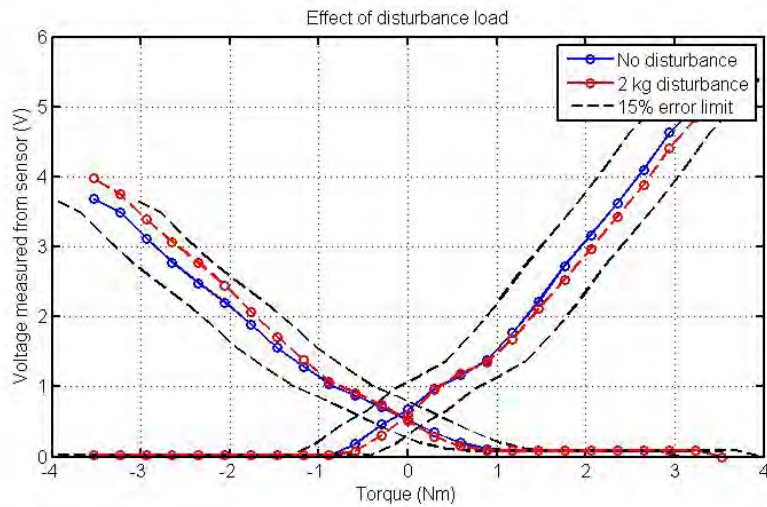
(b) The effect of a disturbance load. In the figure the 15% error bounds are shown as well. The measured error stays well within the bounds.

5.8 Synchronization

The data is collected using three separate systems.

- The data acquisition device NI USB-6211 from National Instruments.

- The Xsens MTI-g orientation sensor.

- The digital video recorder.

Both these device are connected to the Samsung N120 netbook using USB-cables. However starting both measurements at exactly the same time has proven to be difficult. Both measurements are started using Matlab, however Matlab cannot start both systems at the same time. The time between the start of both measurements is between 0.04 and 0.12 sec. This delay depends mostly on the speed of the notebook. Because both systems start at a different time a method for synchronizing both signals is required.

For the purpose of synchronizing the data from de National Instruments data acquisition device and from the MTI-g Xsens orientation sensor a Feteris 400A, 20 G, 1D-acceleration sensor is connected to the data acquisition device. Before each measurement the bicycle is struck with a hammer. This creates a pulse coming from the acceleration sensor that is connected to the data acquisition device. The pulse is also visible in the Xsens acceleration sensor. The pulse in these two measurement signals occurs at the same time since the hammer struck the bicycle only once, this way the measurement data can be synchronized.

To be able to synchronize the video with the measurement results the analog output of the data acquisition device was used in order to send a sinusoidal signal with a frequency of 300 Hz on the audio channel of the digital video recorder, thereby introducing an audible (constant) tone to the recorded audio track of the video. This tone starts playing when the measurement starts and stops when the measurement was stopped. This way the start of the measurement is known and by this each time instant in the measurement data can be related to a corresponding video frame.

Chapter 6

Test subjects

6.1 Groups

An ideal group of test subjects would be the group of people for which the bicycle simulator is intended. That would be in the first place a group of people in physical rehabilitation who for example have lost a limb and now need to relearn riding a bicycle. And maybe a second group of people with a mental disorder. However putting these people on a bicycle would be too risky for approval of any ethical committee.

Also before a bicycle simulator could be used in for example a physical rehabilitation center first different steps would be needed. A possible first appliance of a bicycle simulator could for example be for helping people to learn ride a bicycle during a citizenship education.

In order to get a general idea of the bicycling behavior of people three groups of people have been selected

- Adults (between 18 years old and 55 years old)

- Elderly people (more than 55 years old)

- People who have not yet mastered riding a bicycle

Adults

The reason for having normal adults as a group is to have a control group. Normal adults should be able to ride the bicycle simulator as well as inexperienced cyclists. When an inexperienced rider learns to ride a bicycle his bicycling behavior should start to resemble that of a normal adult more and more. This means that these regular riders are just as much an important group of test subjects as the inexperienced riders.

Elderly people

A factsheet [10] that was published by "Stichting Wetenshappelijk Onderzoek Verkeersveiligheid", which roughly translated means: "Foundation of Scientific Research of Traffic Safety" reveals the following function disorders as a result of the aging process.

- Reduced visual abilities

- Reduced ability to react

- Problems with dividing attention

- Decline of motor system functions

- Slower movements

- Decline of muscle strength

- Decline of the fine coordination

- Relatively strong decline of the ability to adjust to sudden changes in the posture

These function disorders have as a result that elder people have a bicycle behavior that differs from that of younger people.

Although elder people will ride a bicycle differently from people learning or relearning to ride a bicycle, their instability will cause their bicycle behavior to resemble that of people learning to ride a bicycle. Since elder people were abundantly available in contrast with people learning to ride a bicycle, measuring their bicycle behavior seems sensible.

Also the possibility of future usage of the bicycle simulator for elder people should be considered. In that case the bicycle simulator will also be used by elder people.

People who have not yet mastered riding a bicycle

In Delft there are some people who are currently not yet experienced cyclists. Most of them are international PhD-students. This is the most interesting group because the bicycle simulator is meant for adults learning or relearning to ride a bicycle. Since this group should be able to ride the bicycle simulator this seems like a natural choice of test subjects.

6.2 Requirement

Method

In this section the method for determining the number of test subjects is discussed. Prior to the measurements the number of test subjects was unknown.

Because for the design of the simulator the maximum loads, accelerations, velocities and positions need to be known the maximum value for the parameters discussed in chapter 4 need to be determined. Since each measurement produces one extreme value (maximum of the absolute values) is found the mean of these extreme values of the measurements is determined.

For most parameters the absolute value was considered. For example finding the extreme value of the steer angle gives some indication about what would be the maximum steer angle for this person however when designing a bicycle simulator the design will be made symmetric. On the simulator one will be able to steer to the right as much as one will be able to steer to the left. The direction of the maximum for the steer angle is therefore not important, the absolute value is to be considered. This applies to all the parameters, mentioned in section 4.1 except the one parameter, forward acceleration. The forward acceleration depends on the force the rider applies to the pedals. The deceleration however depend largely on the quality of the brakes. For this reason only the maximum value of the forward acceleration is considered and not the minimum value (deceleration).

For example when looking at the steer angle δ for each measurement the maximum of the absolute value of the steer angle of the bicycle was found. The maximum steer angle is found from the data points where the rider is riding the bicycle, not while standing still. These maxima are determined for all riders and from these values a mean value is determined.

Every time a new measurement is added this mean value changes, in order to know the the mean value of everyone exactly one should measure every human being on the planet. Since the number of test subjects is limited to a small value the real mean cannot be found. What can be found however is the range in which the real mean will be with 95% certainty.

The method of determining the range in which the real mean is is called: "the bootstrap". How this method works is explained in the next part of this section.

The bootstrap

Suppose that for the group of elderly people there is a population of approximately 6 million persons in the Netherlands. What if a measurement was done using only 8 test subjects and from these test subject only one parameter was

used, namely the maximum steer torque. The average value from these 8 test subjects is most likely not the same as the average value for the entire population of 6 million. What would be the range in which the true average value would be with a probability of 95%?

Something that should be noted is that the probability distribution of extreme values is usually not a normal distribution. This makes that it is somewhat more difficult to retrieve this range. A statistical method that is often used in such circumstances is the bootstrap method.

Suppose the mean value for the maximum steer torque of the 8 different test subjects is 4.15 Nm. To conclude that the average value of the entire population of 6 million people is 4.15 Nm would be unwise. The reason is that, if a new dataset of steer torques was observed, a different sample mean would be found as an estimate of the average value.

The random values of 8 test subjects : $X_1, X_2, ..., X_8$

The mean value of this sample is found by:

$$\bar{X}_n = \frac{X_1 + X_2 + ... + X_8}{8}$$

The bootstrap principle works by choosing numbers from the previous dataset randomly selecting the numbers. The random numbers are denoted by the symbols $X_1{}^*, X_2{}^*, ..., X_8{}^*$
This dataset is called a *bootstrap random sample*.

The average value of this sample is then found by:

$$\bar{X}_n^* = \frac{X_1{}^* + X_2{}^* + ... + X_8{}^*}{8}$$

This average value is called the *bootstrapped sample mean*. By doing this numerous times iteratively a probability distribution for this mean can be found and thus a 95% probability range.

Example

Suppose the dataset consists of these 8 values. (the absolute value of the torques is considered)

4.1170 5.3484 3.4689 3.8067 4.1450 3.8726 4.3853 4.0786

The probability density function of this sample is shown in figure 6.1.

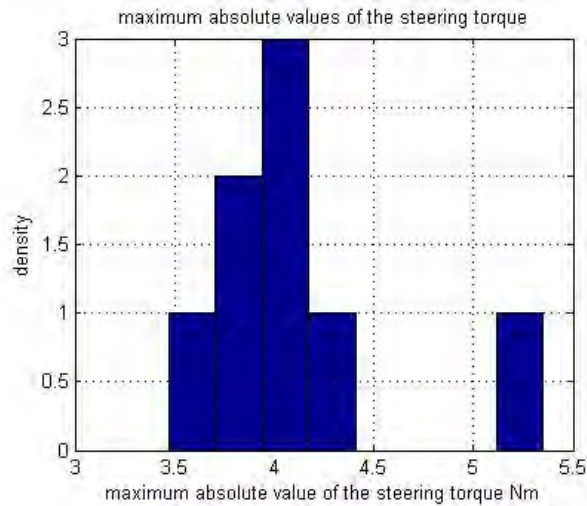Now bootstrap random samples can be generated based on the distribution

Figure 6.1: The probability distribution function of the measured maximum absolute values of the steering torque

function. Note that this is basically the same as choosing random numbers from the original sample. The following Matlab code can be used in order to automate this process and compute the 95% probability range for the mean value of the entire population of 6 million persons.

```
steertorque=[4.1170  5.3484  3.4689  3.8067  4.1450  3.8726  4.3853  4.0786];
bootci(6e6/length(steertorque),@mean,steertorque)
```

The resulting range that is found in less than 20 seconds of calculations:

```
ans =
    3.8843
    4.6582
```

This is 4.27 Nm ± 0.39 Nm. Which is 4.27 Nm ± 9.1 %. Note that the mean of the steer torques (4.15 Nm) is not the same as the mean of the range (4.27 Nm).

The requirement for the number of test subjects is that for each of the parameters the size of the range is less than 20% of the middle value. In this case the range is 4.27 Nm ± 9.1 %, since 9.1%¡20% the requirement is met for this group (elderly people) and for this parameter (the steer torque).

Whenever this criterium is not met; the number of test subjects is insufficient. After each measurement a check was done in order to determine if this requirement was met.

6.3 Number of test subjects

From each group several people were measured.

- 12 Adults were measured

- 9 Elder people were measured

- 2 Inexperienced cyclists were measured

The number of test subjects for the first two groups were chosen carefully, the measurements were continued until the requirements were met. The method for determining if the requirements are met discussed in section 6.2 was executed at the end of every day of measurements.

The last group of test subjects who are inexperienced cyclists proved to be more difficult.

In the Netherlands there are not many people who have not yet mastered riding a bicycle. The international students and PhD students learn riding a bicycle usually shortly after their arrival in the Netherland since it is one of their main means of transport. The amount of people that were currently learning to ride a bicycle were too hard to find to create a proper set of measurements.

Also many international students are shorter than most Dutch people. The bicycle that was used for the measurements is made for Dutch people of average length. One of the inexperienced cyclists that were measured had problems with riding the bicycle since this test subject could not reach the ground with his/her feet. This makes getting on the bicycle tremendously difficult when you are not an experienced cyclist. Also this test subject had problems with going in the right direction. He/she was so concentrated on staying upright on the bicycle that he/she did not think about going left or right. As a result the route that was taken was a route that was different from the route that was taken with the other test subjects.

One of the measurements with an inexperienced cyclist was canceled because it seemed too dangerous to proceed. This test subject also could not reach the ground with his/her feet although the saddle was lowered to the lowest possible position. The fact that this test subject could only get on the bicycle caused him/her to indicate that it would be safer not to do the measurement. Even if this test subject could be able to start and ride the bicycle without falling, stopping without falling would be a problem. This seemed unsafe and the measurement was stopped before the start.

Chapter 7

Measurement protocol

First several things about the test subject were registered in order to be able to contact them later and the weight for calculation purposes. Also a question was asked about the bicycle experience and the age of the test subject in order to be able to know in which group the test subject belongs.

- His/her name

- phone number

- age

- bicycle experience experienced / average / beginner

- weight

Then for each measurement, first, if necessary, the height of the saddle is adjusted. Next the video recorder is started. Next the measurement is started in Matlab. This means that the mini notebook is collecting data from the Xsens sensor and the data acquisition device.

Also from the start of each measurement the data acquisition device is creating a tone on the audio channel of the digital video recorder. This is just in order to be able to know at which point in the video the measurement is started. This is explained in further detail in section 5.8.

Next the bicycle frame is struck with a hammer. This is to be able to synchronize the data from the MTI-g orientation sensor with the data from the data acquisition device. This is necessary because starting both measurements at the same time has proven to be difficult. Striking the frame with a hammer will create a large peak in the accelerometer signals from both signals and this is used as a reference mark for the start of the measurement. Also this is explained in further detail in section 5.8.

Then the rider is asked to climb on the bicycle. The strap of the helmet is adjusted and the rider puts on the helmet. Then the rider puts on the backpack and then the arm that connects the potentiometer with the backpack is installed on the bicycle. The orientation of this arm is different for each measurement.

Lastly the rider is given directions at every turn by the person doing the measurements who rides with the test subject on a different bicycle.

Chapter 8

Measurement data

8.1 Filtering

Expected frequency range

Measured data is often not a smooth signal. The surroundings always have an effect on the measurement equipment. Also the measured device is being influenced by small disturbances. The measured data often contains disturbances of many frequencies. In the case of the measurement bicycle the frequencies of the movements of the bicycle are known to be below a certain limit.

Modeling a controlled bicycle is difficult and much research needs to be done before a reliable model can be made of this. The model for the uncontrolled bicycle however is already described in section 3.2. In this section equation 3.1 was mentioned. This is the differential equation that governs the movements of the bicycle.

$$M\ddot{q} + vC_1\dot{q} + [K_0G + v^2K_2]q = f \qquad (3.1)$$

The homogenous solution to this differential equation gives the motion of the uncontrolled bicycle. Therefore f is assumed zero. Furthermore assuming $q = ce^{\lambda t}$ the equation becomes the following.

$$\left\{ M\lambda^2 + vC_1\lambda + [K_0G + v^2K_2] \right\} ce^{\lambda t} = 0 \qquad (8.1)$$

This is only possible if.

$$M\lambda^2 + vC_1\lambda + [K_0G + v^2K_2] = 0 \qquad (8.2)$$

This equation is solved in Matlab using the following command.

```
polyeig(K0*g+v^2*K2,v*C1,M)
```

Since the results are dependent of the forward speed of the bicycle v this was done for all speeds from 0 to 10 m/s. The matrices that were used and some
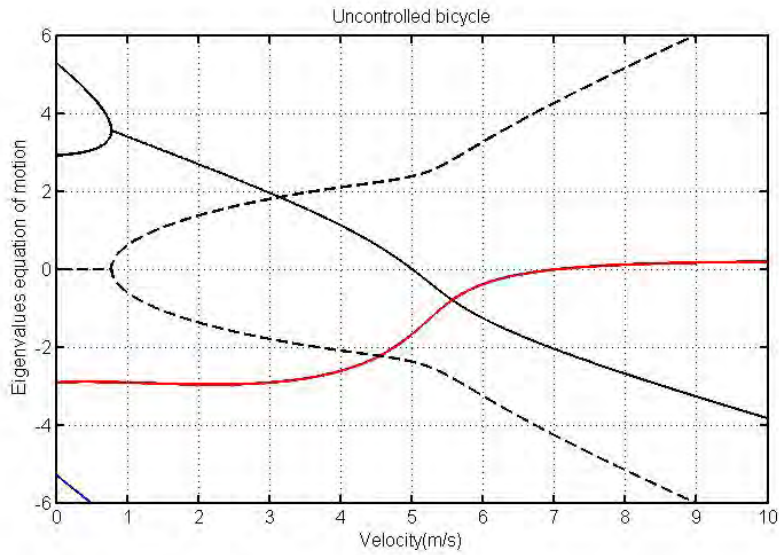
Figure 8.1: The eigenfrequencies of the uncontrolled bicycle. The complex eigenfrequencies are shown with dotted lines, presence of complex eigenfrequencies indicate oscillations, presence of positive real eigenfrequencies indicate instability

parameters of the measurement bicycle are shown in section A.2. The eigenvalues are shown in figure 8.1.

Since figure 8.1 shows the solutions of equation 8.1 the values of λ are shown in the figure. A complex value (shown with dotted lines) indicates oscillations. A negative real value indicates a stable motion and a positive real value indicates unstable motion.
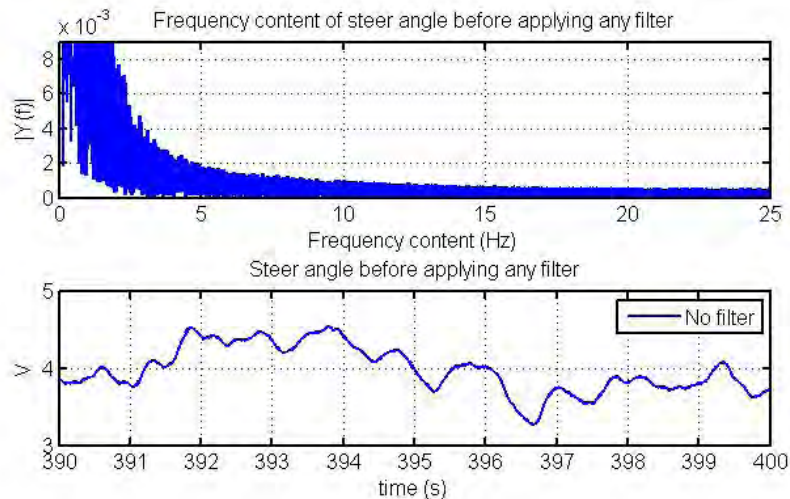
Figure 8.2: The measured data from the steer angle before applying any filter.

Type of filter

Before filtering

As was mentioned before the real frequency content of the data includes many disturbances. The frequency content is shown in figure 8.2.

Lowpass Filter

When selecting a type of filter for the data one should take care to preserve the low frequency oscillations that occur while riding this bicycle. The goal is that the higher frequencies are all removed. A lowpass filter was therefore used. The cutoff frequency of the filter was set to 4 Hz in order to be sure the oscillations caused by the bicycle are preserved.

The frequency content of the data after filtering with a regular lowpass filter along with an example of the data before and after filtering is shown in figure 8.4(a). The figure shows a time shift between de filtered and the unfiltered data. This is caused by the phase shift that the filter imposes on the data.

Zero phase lowpass filter

The time shift shown in figure 8.4(a) is unwanted. The standard *filter* command in Matlab can be replaced by the *filtfilt* command. This command filters the data with a zero phase lowpass filter. This filter gives a similar result but without the time shift. The frequency content of the data after filtering with

a zero phase lowpass filter along with an example of the data before and after filtering is shown in figure 8.5(a). In this figure can be seen that the frequency content is no longer cut off at 4 Hz. This is a result of the time shift. The filter works in largely the same way as the regular lowpass filter though.
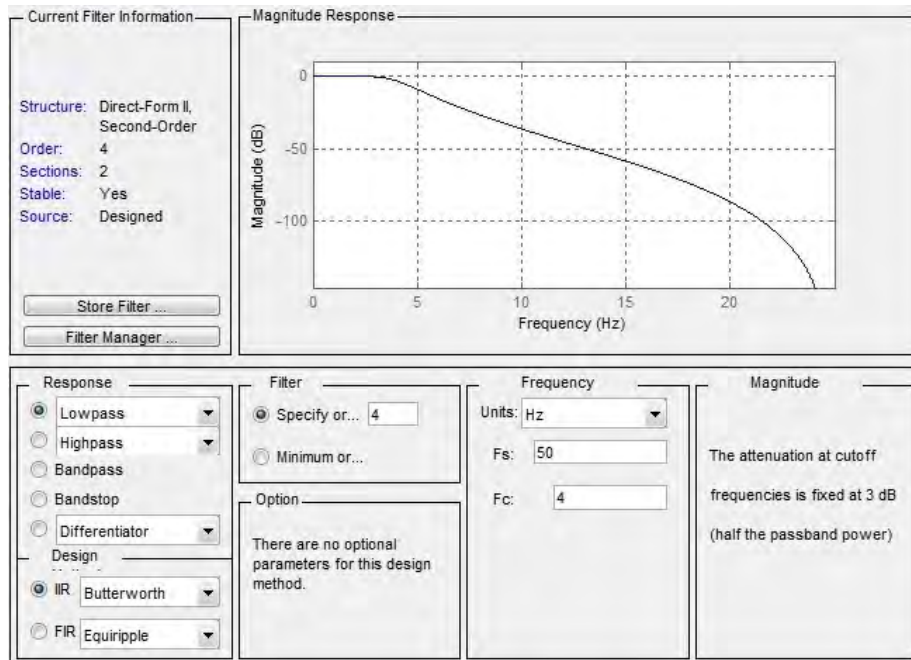
Figure 8.3: The options that were chosen for the lowpass filter in the "Filter Design and Analysis Tool" which is included in the filter design toolbox by Matlab. The frequency response function is shown as well
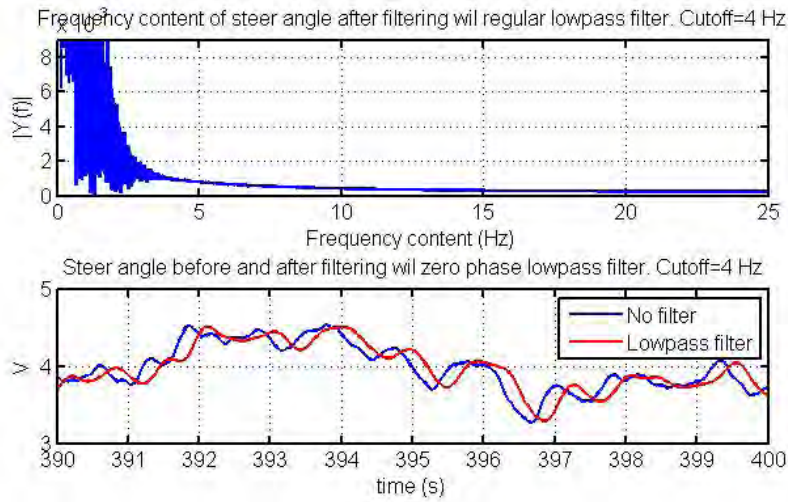
(a) The data from the steer angle after applying a regular lowpass filter with a cutoff frequency of 4 Hz.

Figure 8.4:
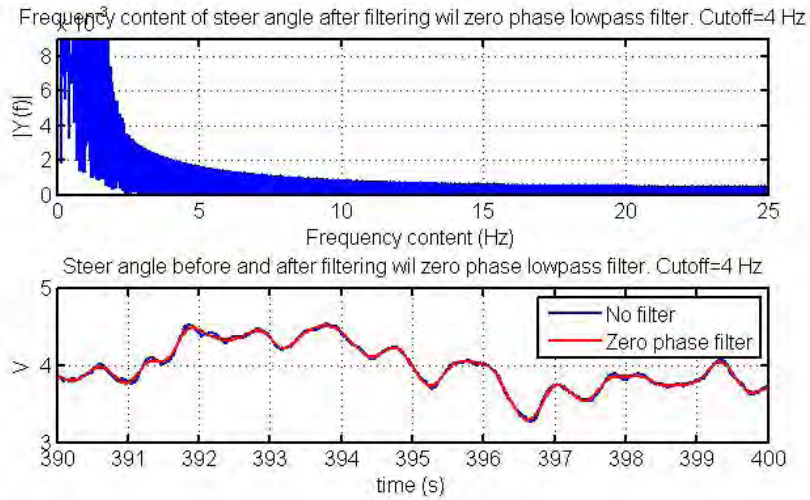
(a) The data from the steer angle after applying a zero phase lowpass filter with a cutoff frequency of 4 Hz.

Figure 8.5:

8.2   Measurement data

In this section an impression of the measurement data will be given. The complete dataset will be shown for one person.

Route

The route that was taken was carefully selected in order to meet the following criteria.

- Start and stop at the 3mE faculty since all the test subjects are from this faculty. Also the square at the front entrance provides a place where the rider can get on and off the bicycle safely. This usually takes 5 to 10 minutes.

- Include many curves since added duration of all straight parts will always be greater than the added duration of all curves. Straight parts provide valuable data however curves provide valuable data as well.

- Include at least one traffic light. Measurements of stopping and starting are valuable.

- Include a roundabout, this provides a circular path for the rider to follow which is different from normal curves and straight parts.

- Include crossing the road often so the rider needs to pay attention to the traffic.

- Avoid getting near large buildings since the orientation sensor requires a GPS-signal. Large buildings can block the GPS-signal.

- Include a number of speed bumps, the response of the test subject could provide valuable data.

The route that was taken is shown in figure 8.6(a). This data is measured by the GPS that is included in the MTI-g orientation sensor. The figure also shows a red line (a left curve). This is the part that is shown in the other figures in this section.

The accuracy of the measured position is 2.5 m provided that GPS fix is available throughout the measurement. For this measurement the GPS-fix is constant. This is also true for most of the other measurements.

When approaching faculty of Electrical Engineering of the Technical University of Delft in some cases the GPS signal was lost because of the tall building being in the vicinity of the GPS receiver. Loss of GPS fix has a duration of normally no more than 3 seconds. Losing GPS fix for longer than 1 minute can have a noticable result on the measured orientation by the MTI-g orientation

sensor because the GPS signal is used along with other data to find the sensor's orientation using a Kalman filter.
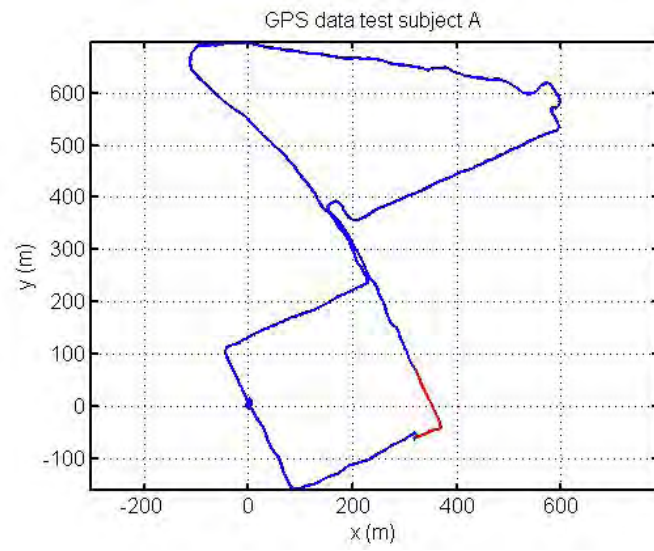
(a) Measured data from the GPS. Test subject A

(b) Measured data from the GPS shown in google maps. Test subject A.

Figure 8.6:

Orientation sensor data

The output from the MTI-g orientation sensor is shown below. The red line in figure 8.6(a) indicates which part is shown in the figures. Figure 8.7(a) shows the measured orientation of the sensor. Figure 8.7(b) shows the output from the accelerometer in the MTI-g sensor. Data from the rate gyroscope and the magnetometers of the MTI-g sensor are shown in respectively figure 8.8(a) and figure 8.8(b).

Orientation

The roll angle shows a noticeable dip of $-11°$. This is caused by the bicycle going through the (left) curve shown in figure 8.6(a). The yaw angle changes from $-78°$ to $25°$. The pitch angle which should show only small changes caused by small bumps in the road stays between $-4°$ and $-1°$, this is partly due to the dynamic accuracy of the sensor $\pm 1°$.
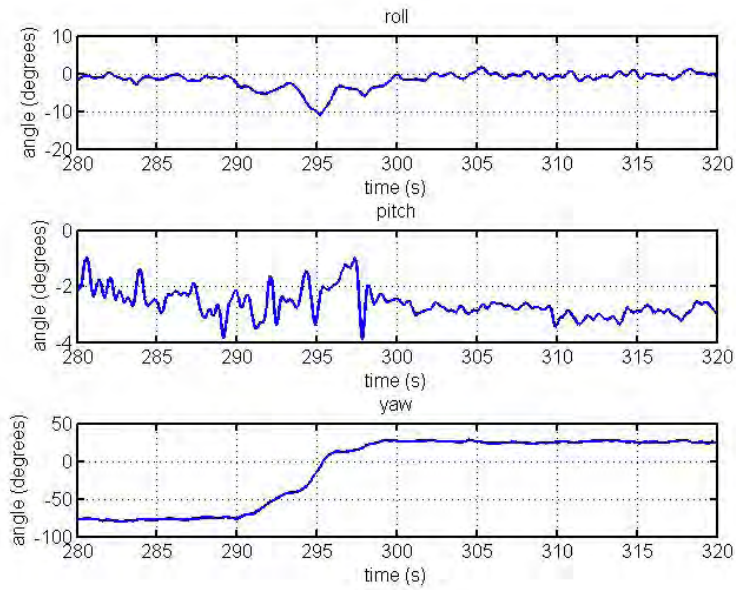
Acceleration

The acceleration shows no noticeable changes at the time instant were the bicycle goes through the curve (t=290 sec to t=300 sec). One would expect to see changes in the acceleration at the time of the curve caused by the centripetal acceleration of the bicycle. Why this is is explained in section 8.2.

Rotation speed

The gyroscope signal shows a dip and then a peak at the time of the curve (t=290 sec to t=300 sec) in the rotation speed around the x-axis which is the same as the angular velocity in the roll direction of the bicycle. This is due to the decrease of the roll angle and then again an increase of the roll angle when the bicycle is accelerating out of the curve.

Magnetometer

At the time of the curve (t=290 sec to t=300 sec) the signal from the magnetometers of the MTI-g orientation sensor shows an increase from the magnetometer x-direction and a decrease of signal from the magnetometer in y-direction. This is due to the fact that before the curve the heading of the bicycle is in south-east-east direction and after the curve the bicycle is moving in north-north-west direction.

(a) Measured orientation from the orientation sensor located on the luggage carrier of the bicycle. Test subject A.
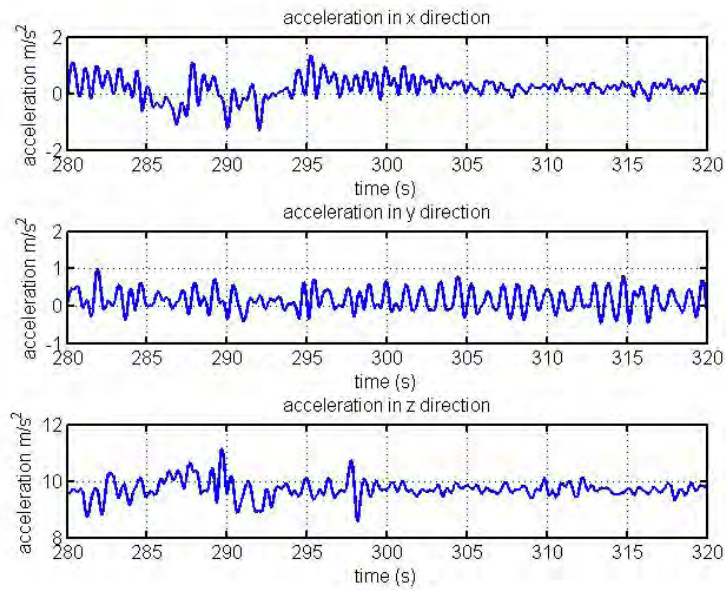
(b) Measured acceleration from the orientation sensor located on the luggage carrier of the bicycle. Test subject A

Figure 8.7:
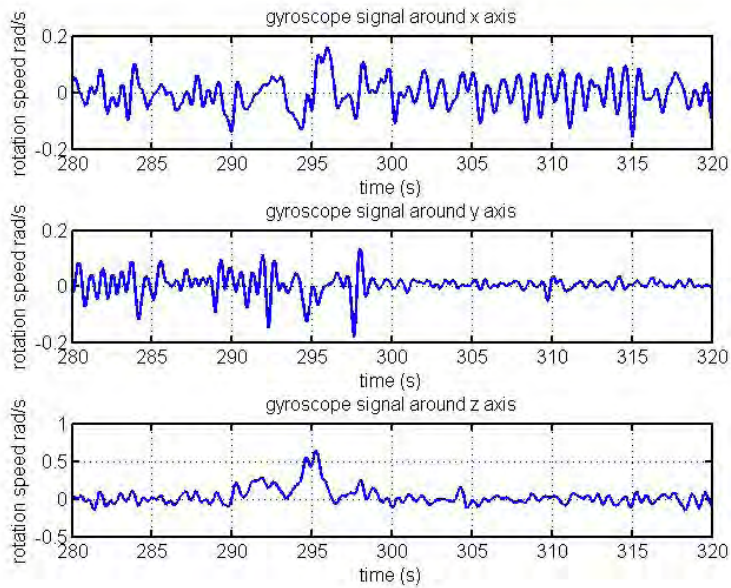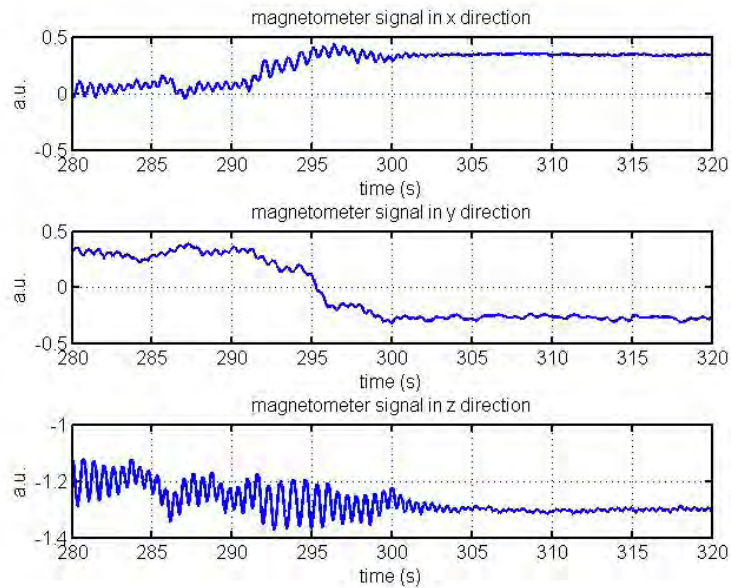
(a) Measured angular velocity from the orientation sensor located on the luggage carrier of the bicycle. Test subject A.

(b) Measured magnetic field strength from the orientation sensor located on the luggage carrier of the bicycle. Arbitrary units are shown because the signal is normalized with the earth's magnetic field. Test subject A.

Figure 8.8:

Data acquisition device data

The output from the national instruments data acquisition device is shown below. The red line in figure 8.6(a) indicates which part is shown in the next set of figures.

Cadence

Figure 8.9(a) shows the cadence frequency. How this sensor works is described in section 5.4. A dip in the measured voltage means that at time instant the pedal is near the sensor. The time between the dips (T) can be used in order to determine the cadence frequency using the relation $F = \frac{1}{T}$.

Steering torque

Figure 8.9(a) also shows the steering torque that the rider exerts on the handlebars. Detailed information about the torque sensor is provided in section 5.7. The amplitude of the actuation is different on the straight parts (t=280 sec to t=290 sec and t=300 sec to t=320 sec) from the amplitude of actuation in the curve (t=290 sec to t=300 sec). At the time of the curve steering torques with a larger amplitude are measured.

Body movement

Lastly the body movement of the rider relative to the bicycle is shown in figure 8.9(a). Detailed information about the measurement system of the lean angle of the rider relative to the bicycle is provided in section 5.3. The arm connecting the potentiometer and the backpack of the rider is connected at the start of each measurement. This means that the angle of the potentiometer can accurately be measured however the orientation of the arm can be different for each measurement. This means that the actual position of the rider during the measurement is not known however the relative changes are known. Therefore the assumption is made that while riding the measurement bicycle the average lean of the rider relative to the bicycle should be zero. In the figure can be seen that the movements of the rider during the curve (t=290 sec to t=300 sec) is small relative to the movements of the rider on the straight parts (t=280 sec to t=290 sec and t=300 sec to t=320 sec). This is due to the fact that the rider is pedalling on the straight parts and he stops pedalling when approaching the curve. This is characteristic for all riders.

Speed

The speed of the bicycle, measured at the bicycle's rear wheel is shown in figure 8.9(b). Detailed information about the electric motor measuring the forward speed of the bicycle is provided in section 5.1. The speed shows a decrease of the speed while approaching the curve (t=280 sec to t=290 sec) as the rider

stops pedalling and then an increase as the rider is accelerating out of the curve (t=300 to t=320).

Steering angle

The steering angle of the bicycle is also shown in figure 8.9(b). Detailed information about the potentiometer measuring the steer angle of the bicycle is provided in section 5.2. At the time of the curve (t=290 sec to t=300 sec) a temporary decrease of the steer angle to $-16.25°$ is visible. This is correct because this is a left curve, a steer angle to the right is defined to be positive and consequently steering to the left means the steer angle is negative.

Accelerometer

The signal from the accelerometer is shown in figure 8.9(b). Please note that this sensor is not calibrated, this is not required since the only purpose of this sensor is synchronization of both measurement systems. Synchronization of both systems is described in section 5.8.
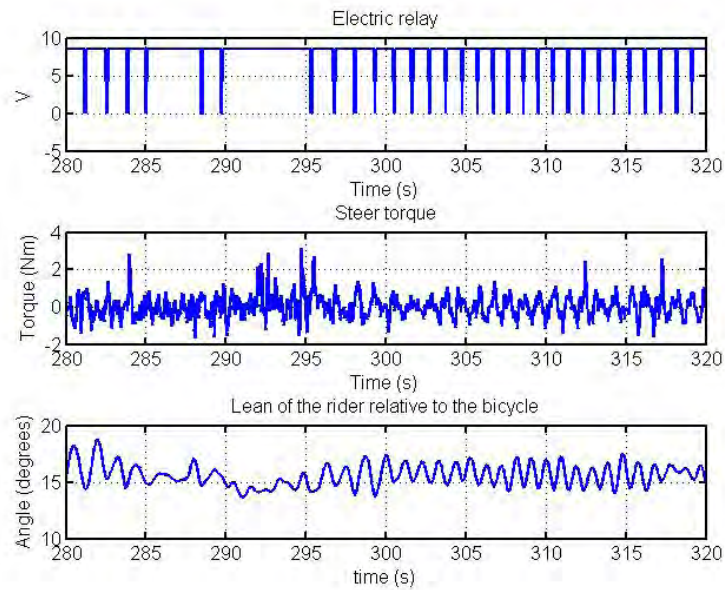
(a) Measured data from the data acquisition device. Test subject A.
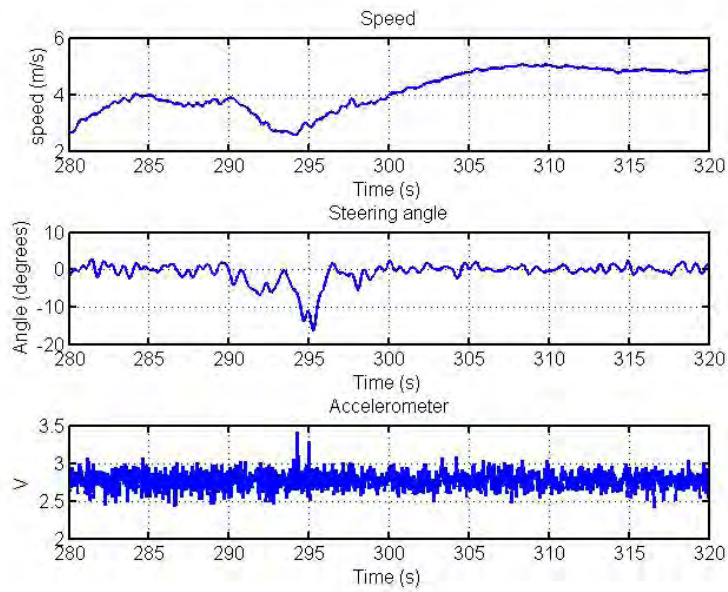
(b) Measured data from the data acquisition device. Test subject A.

Figure 8.9:

61

Calculated data

Several parameters that were calculated using data from the sensors are shown below. The red line in figure 8.6(a) indicates which part is shown in the figures.

Angular velocity in the yaw direction

Figure 8.10(a) shows the angular velocity in the yaw direction (heading). In order to find this angular velocity, data from the gyroscope signals of the MTI-g sensor was used. This data is shown in figure 8.8(a). Next, the orientation output of the sensor was used in order to rotate the gyroscope signal such that it shows the angular velocity of the heading.

The maximum value in this small interval is 0.7 rad/s, please note that this is larger than the maximum of the measured rotation speed around the rotated z-axis shown in figure 8.8(a) which is 0.65 rad/s.

Angular acceleration in the yaw direction

Figure 8.10(a) shows the angular acceleration in the yaw direction (heading). This acceleration was found by differentiating the angular velocity in the yaw direction with respect to time which is shown in the same plot.

Angular acceleration in the roll direction

The angular acceleration in the roll direction is calculated by differentiating the angular velocity signal with respect to time which is measured by the gyroscope of the MTI-g sensor. The gyroscope signal around the x axis is the same as the angular velocity in the roll direction. The data from the gyroscope is shown in figure 8.8(a).

Angular jerk in the roll direction

The angular jerk in the roll direction is calculated by differentiating the angular acceleration in the roll direction with respect to time. This angular jerk is also shown in figure 8.8(a).

Centripetal acceleration

The centripetal acceleration is calculated using the relation.

$$a_{cp} = \frac{v^2}{r} \tag{8.3}$$

In which v is the forward speed of an object and r is the radius of rotation of the object. Since r is unknown, the general relation $\omega = v/r$ is used for the heading of the bicycle. The relation is written in the following form.

$$a_{cp} = \dot{\psi} \cdot v \tag{8.4}$$

In which $\dot{\psi}$ is the angular velocity of the heading ψ.

In the figure the centripetal acceleration caused by going through the curve (t=290 sec to t=300 sec) is noticeable with a maximum amplitude in this small interval of $1.99 m/s^2$ at t=295.3 sec. This is nowhere near the lateral acceleration measured by the accelerometer of the MTI-g orientation sensor which is $0.34\ m/s^2$ at that time.

This can be explained by looking at the roll angle of the bicycle at that time instant. Figure 8.11 shows a rider on a bicycle while going through a curve. The direction of the accelerations as they are measured by the accelerometer are shown.

There is a second acceleration component that is measured by the accelerometer. This is not a real acceleration however. This measured acceleration is just a result of the way the accelerometer measures acceleration. Gravity acts on the accelerometer and due to gravity the seismic mass inside the accelerometer is pulled down. This corresponds to a acceleration is upward direction for the acceleration sensor. This causes the accelerometer to measure a constant acceleration in upwards direction of $9.81\ m/s^2$ even though the accelerometer does not accelerate in upward direction.

A short summary of the different measured parameters at the time instant where the roll angle on this small time interval is maximal which occurs at t=295.3 sec.

Parameter	Symbol	Value
acceleration in the y-direction of the sensor	a_x	$0.1565\ m/s^2$
centripetal acceleration	a_{cp}	$1.985\ m/s^2$
roll angle	ϕ	$-10.74°$

Table 8.1: Values are of test subject A at t = 295.3 sec

A quick calculation shows the lateral acceleration that of the sensor. Note that g is in the equation, this is due to the effect explained above, the sensor measures an acceleration in upwards direction although it does not accelerate in that direction.

$$g \cdot \sin(\phi) + a_{cp} \cdot \cos(\phi) = 0.1221 \frac{m}{s^2}$$

This is relatively close to the measured lateral acceleration of the sensor 0.1565 m/s^2. The relatively small difference could be caused by vibrations due to bumps in the road.
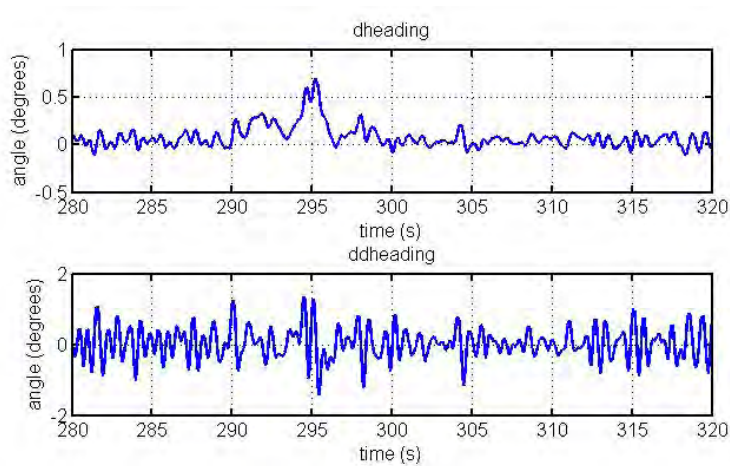
(a) The angular velocity and the angular acceleration of the orientation of the bicycle in the yaw angle direction. In this report referred to as respectively $\dot{\psi}$ and $\ddot{\psi}$. Test subject A.
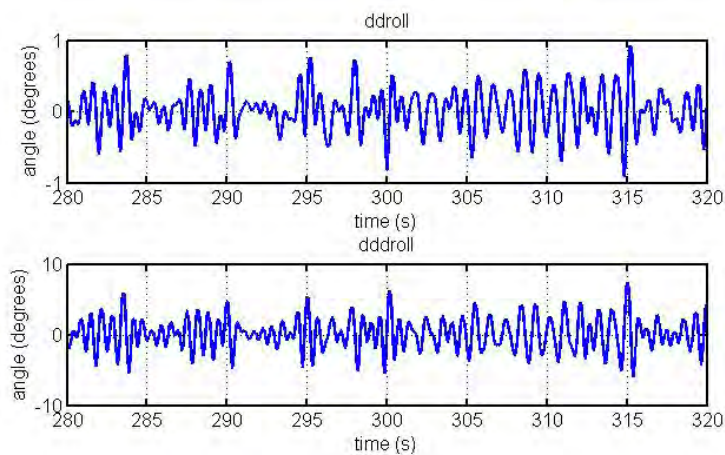
(b) The angular velocity and the angular acceleration of the orientation of the bicycle in the roll angle direction. In this report referred to as respectively $\dot{\phi}$ and $\ddot{\phi}$. Test subject A.
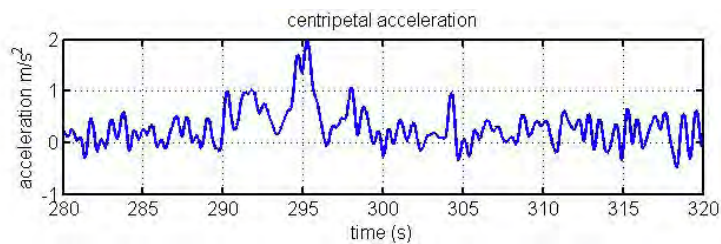
(c) The centripetal acceleration of the bicycle and rider. In this report refereed to as a_{cp}. Test subject A.

Figure 8.10:
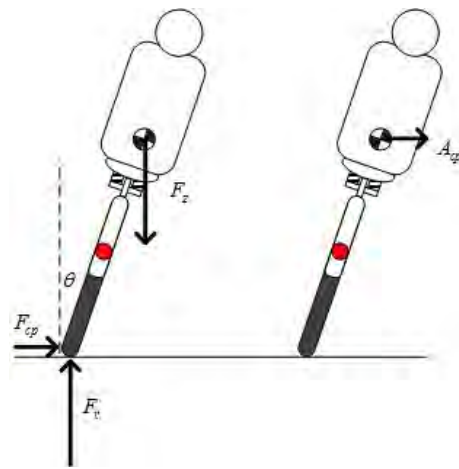
Figure 8.11: The rider on the bicycle, on the left the forces that act on the bicycle and rider are shown. On the right the measured accelerations are shown.

8.3   Video synchronization

When analyzing the measurement results it can come in handy to known what exactly happened at certain time instants. The rider responds to many disturbances from the outside. For example a rapidly approaching cyclist from the right could make the rider use his brakes and so on. On a video such an event can be seen This is why a camera was used in order to record the measurement. More about the camera and the recorder is explained in section 5.5.

Since a video was made it is useful to be able to compare the video with the data. A convenient way of comparing data with video frames is by creating a user interface which synchronizes the data with the video. This way the data can be shown alongside with the video. This interface was created using the GUI builder in Matlab named GUIDE.

The method of synchronization of the video and the measured data is explained in section 5.8. The tone that is played on the audio channel is recoded by the digital video recorder. Each video file was converted after the measurements, the videos were split into an .avi file with only video frames and a .wav file with only audio. This is done because Matlab is unable to read audio from video files. The video synchronization program is able to read the audio file and find the exact time in the video where the measurement is started.

The interface that shows the video synchronized with the data is shown in figure 8.12. The text field in the upper left shows the location and the filename of the data file containing the measured and calculated data. In this case multiple measurements are contained in the data file.

After pressing the button, 'read .mat' the popup lists below the button can be used. The first list is used for selecting the test subject from the test subjects that were contained in the data file.

The second list is used for selecting the variable to plot, this can either be a measured value such as, the steer torque, roll angle, angular velocity in the roll direction etc. It can also be a calculated parameter however such as for example the centripetal acceleration of the rider.

Next, the name of the video file is required in the next text field. Lastly the name of the audio file is required so that Matlab is able to find the exact time instant in the video where the measurement is started.

After pressing the button 'Read video and audio' the start of the measurement is found and the number of frames are determined. Next all video frames are read and resized in order to fit in the computer's memory if necessary. The progress is shown in the text that appears below the button. Then this task is completed the video can be viewed using the slider at the bottom of the inter-
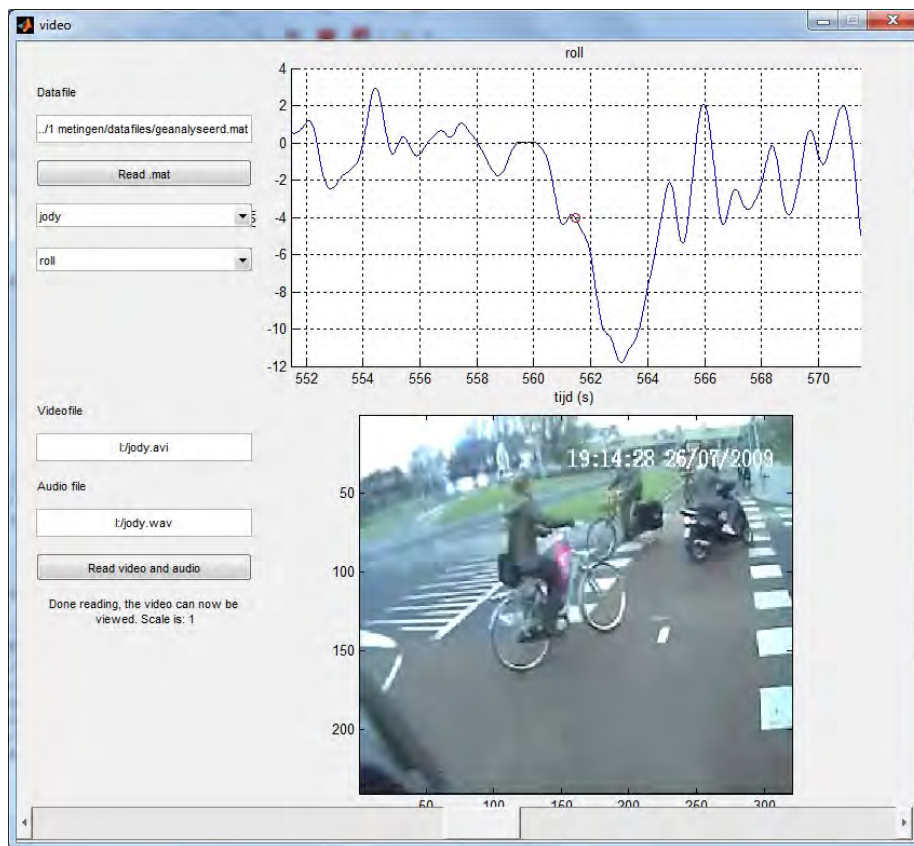
Figure 8.12: The interface created in Matlab showing data synchronized with the video. In this figure the roll angle of an arbitrary rider is shown.

face. The red circle in the plot at the top shows the current value of the data belonging with the video frame that is shown.

It is also possible to instantly selected a different variable to be plotted. When this is done the data in the upper window is instantly replaced with the new variable.

All the videos have been converted using a video converter called 'Portable media coder'. This is convenient since this converter is portable and therefore does not require installation. The settings that were used to convert the video are shown below. Note that these settings have been chosen carefully in order to reduce loading time in Matlab. The lower the resolution and the lower the frame rate is of a video, the faster that video can be loaded into the computer's memory by Matlab.

Setting	Value
Enable audio	Off
Mode	Quality based
Format	XviD
Container	AVI
Resize	On 320 x 240
Frame rate	5

8.4   Test heading

Applying tests to the measured data gives some indication about the reliability of the measured data. A way of testing the measured speed of the bicycle and the measured heading of the bicycle together is making use of equation 3.3 which was mentioned in section 3.2.

$$
\dot{x}^* = v \cdot \cos\psi \\
\dot{y}^* = -v \cdot \sin\psi
\tag{3.3}
$$

The yaw angle that was measured by the MTI-g orientation sensor is now combined by the speed of the bicycle which was measured by the electric motor that was installed on the bicycle. Integration of $\dot{x}^*$ and $\dot{y}^*$ gives a position x^* and y^* relative to the starting point of the bicycle.

This position in x and y can then be compared with the coordinates measured by the GPS from the MTI-g orientation sensor. The y coordinate can be found making use of the earth's radius (6371 km) and the latitude angle.

$$
y_{gps} = \tfrac{latt}{180}\pi \cdot r_{earth}
\tag{8.5}
$$

In order to find the x-coordinate the radius about which the longitude angle is defined needs to be found.

$$
r_{circle} = r_{earth} \cdot \cos\left(\tfrac{latt}{180}\pi\right) \\
x_{gps} = \tfrac{lon}{180}\pi \cdot r_{circle}
\tag{8.6}
$$

The trajectory of the GPS-coordinates transformed in x- and y-coordinates is shown in figure 8.6(a). The trajectories of x^* and y^* and x_{gps} and y_{gps} together are shown in figure 8.13.

The figure shows that the trajectories look similar to a certain extend, this is a relatively good result which indicates the reliability of the measured data. The calculated x^* and y^* seem to be similar at the beginning of the exercise however in the end the starting point is not at the same location as the end point. This is due to small errors in the yaw angle (heading) measured by the MTI-g orientation sensor. These small errors have a large effect on the calculated position at the end of the measurement because throughout the measurement the same error is integrated and therefore the error grows. This relatively small error is most likely caused by misalignment of the MTI-g orientation sensor.
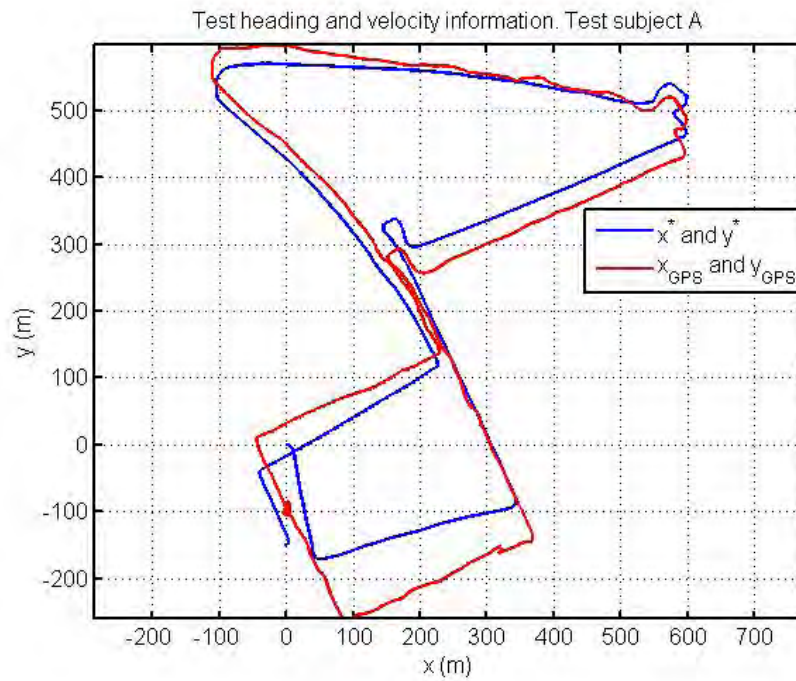
Figure 8.13: The trajectory of x and y calculated from the heading of the bicycle together width the heading of the bicycle, shown as respectively x^* and y^*, together with the position measured by the GPS, shown as x_{gps} and y_{gps} . This is done for an arbitrary rider.

8.5 Test steer angle

Applying tests to the measured data gives some indication about the reliability of the measured data. A way of testing the measured steer angle is making use of equation 3.2.

$$\dot{\psi}^* = \frac{\delta v + \dot{\delta} c}{w} \cos \lambda \tag{3.2}$$

In which $\dot{\psi}^*$ is the angular velocity with which of the yaw angle (heading) of the bicycle. δ and $\dot{\delta}$ are respectively the steering angle and the angular velocity of the steering angle. v, c, w and λ are respectively, the speed of the bicycle, the trail of the bicycle, the wheel base of the bicycle and the steer axis tilt of the bicycle.

The properties of the bicycle that was used were found earlier, they are mentioned in the paper written by A.L. Schwab [3] that was mentioned earlier. They are shown in table 8.2.

Table 8.2: Parameters of the bicycle used in the model.

Parameter	Symbol	Value
Wheel base	w	1.121 m
Trail	c	0.0686 m
Steer axis tilt	λ	22.9°

The angular velocity of the bicycle in the direction of the yaw angle calculated using relation 3.2 is shown in figure 8.14(a). The actual angular velocity of the bicycle in the direction of the yaw angle is shown as well. The figure shows that these two signals are similar which shows the reliability of the measured data.

The quantity $\dot{\psi}^*$ is transformed into ψ^* by integrating $\dot{\psi}^*$ numerically. The calculated yaw angle (heading) ψ^* is shown together with the heading measured by the MTI-g orientation sensor, ψ in figure 8.14(b).

71
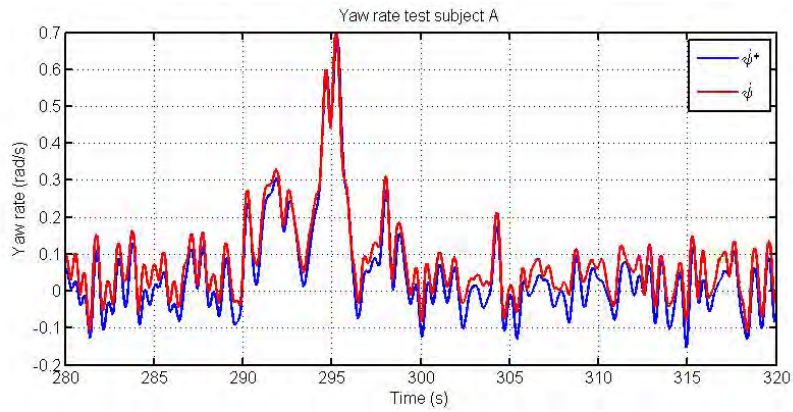
(a) The angular velocity of the bicycle in the direction of the yaw angle. In this figure this yaw rate was calculated using relation 3.2 is shown as $\dot{\psi}^*$. The yaw rate calculated from the gyroscope data is shown as $\dot{\psi}$.
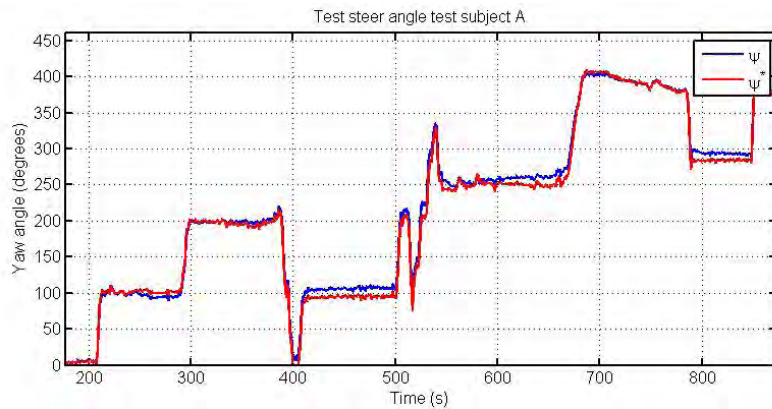
(b) The the heading measured by the MTI-g orientation sensor and the heading calculated making use of only the steer angle shown in one figure. In the figure these parameters are named respectively ψ and ψ^*.

Figure 8.14:

72

8.6 Test applied torques

Applying tests to the measured data gives some indication about the reliability of the measured data. A way of testing the measured steer angle is making use of equation 3.1, which was mentioned and explained before in section 3.2.

$$M\ddot{q} + vC_1\dot{q} + [K_0g + v^2K_2]q = f \tag{3.1}$$

In which $q = \begin{bmatrix} \theta & \delta \end{bmatrix}^T$ and $f = \begin{bmatrix} T_\theta & T_\delta \end{bmatrix}^T$. This equation can be used to calculate the torques that were applied to the bicycle T_ϕ and T_δ. T_ϕ is the torque that the rider applies to the bicycle directly by moving his center of mass. T_δ is the torque that the rider applies to the handlebars, the steering torque.

The different parameters that are contained in the equation were found in the following way.

- ϕ, the lean angle of the bicycle, this parameter was measured by the MTI-g orientation sensor.

- δ, the steer angle of the bicycle, this parameter was measured using the potentiometer described in 5.2.

- $\dot{\phi}$, the angular velocity in the roll direction, this parameter was measured by the MTI-g sensor using a gyro-sensor.

- $\dot{\delta}$, the angular velocity of the handlebars in the steer angle direction. This parameter was found by differentiation of δ with respect to time.

- $\ddot{\phi}$, the angular acceleration in the roll direction. This parameter was found by differentiation of $\dot{\phi}$ with respect to time.

- $\ddot{\delta}$, the angular acceleration of the handlebars in the steer angle direction. This parameter was found by differentiation of $\dot{\delta}$ with respect to time.

- v, the velocity of the bicycle, measured by the electric motor described in section 5.1.

The result of applying equation 3.1 is the two torques T_ϕ and T_δ. First of all the calculated torque applied to the handlebars, T_δ is compared to the steer torque that was measured directly by the sensor described in section 5.7. These two torques are shown in figure 8.16(a). In the figure can be seen that the difference between these two signals is relatively small.

The lean angle of the rider relative to the bicycle is measured using the arm and potentiometer discussed in section 5.3.

The rider applies a torque by moving his upper body. The mass and the location of the center of mass of the upper body of test subject A is approximated using data mentioned in an a paper [2] written by Jason K. Moore, Mont Hubbard,

73

A. L. Schwab, J. D. G. Kooijman. The calculations were done using Matlab. In this calculation the assumption was made that the upper body while rotating stays rigid and that the upper body consists of: the torso, the head and the upper arms. The lower arms are assumed not to move since the rider is holding the handlebars.

Since the torque that is caused by the weight of the rider and by the weight of the bicycle as a result of the roll angle of the bicycle is already incorporated in the model described by equation refeq:bicycle the angle relative to the bicycle will be used. Since the torque that the rider applies to the bicycle due to gravity when the rider stays in plane with the bicycle is already incorporated into the model, the torque that the rider applies by moving relative to the bicycle will be calculated as if the bicycle were in upright position.

The resulting mass and height of the center of mass of the upper body of test subject A are shown in table 8.6

Parameter	symbol	Value
mass upper body	m_u	52 kg
height of center of mass (measured from saddle)	h_u	0.9546 m

Table 8.3: Properties for test subject A which were calculated using data from the paper [2] that was mentioned earlier

When the rider moves his upper body the displaced center of mass exerts a torque due to gravity and the rider also applies a torque to the bicycle in order to move his/her body. This torque along is shown in figure 8.15.

The resultant torque is calculated in the following way

$$T_{\phi 2} = m_u \cdot h_u \cdot g \cdot \sin(\phi_r) - I \cdot \ddot{\phi}_r \qquad (8.7)$$

In which m_u is the mass of the upper body of test subject A. h_u is the height of the center of mass of the upper body measured from the top of the seat. ϕ_r is the lean angle of the rider that is measured by the potentiometer. I is the moment of inertia, given by: $I = m_u \cdot h_u^2$. $\ddot{\phi}_r$ is the angular acceleration of the lean angle of the rider.

The calculated torques T_ϕ and $T_\phi 2$ are shown in figure 8.16(b).
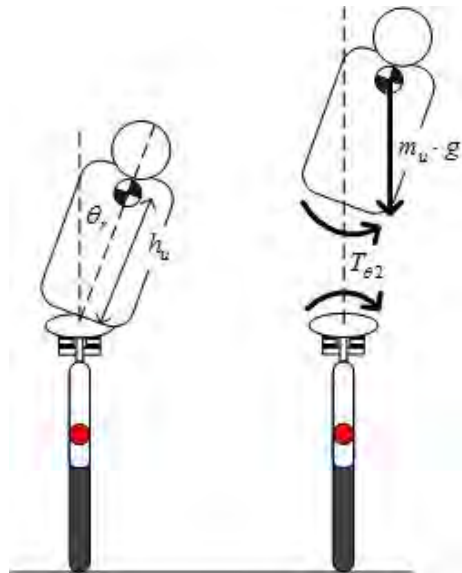
Figure 8.15: The rider on the bicycle, this figure shows what the relative angle means the torque that is calculated by equation 8.7 is illustrated as well
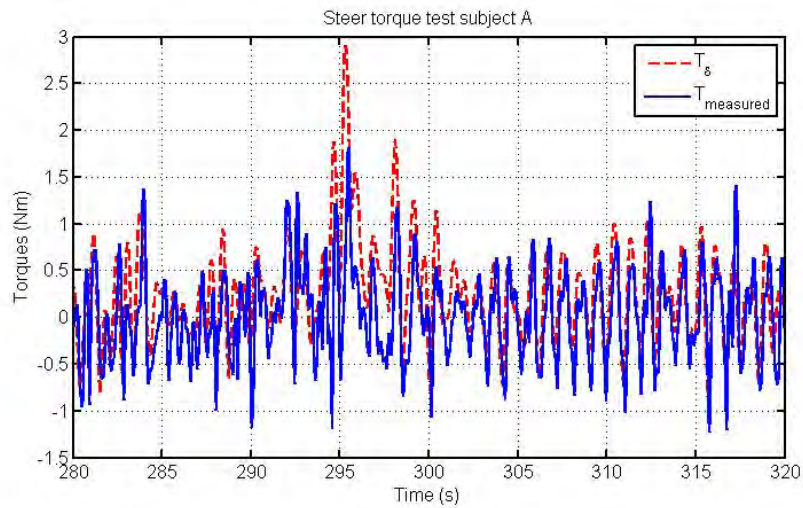
(a) The calculated steering torque, referred to as T_δ, along with the measured steering torque, referred to as $T_{measured}$
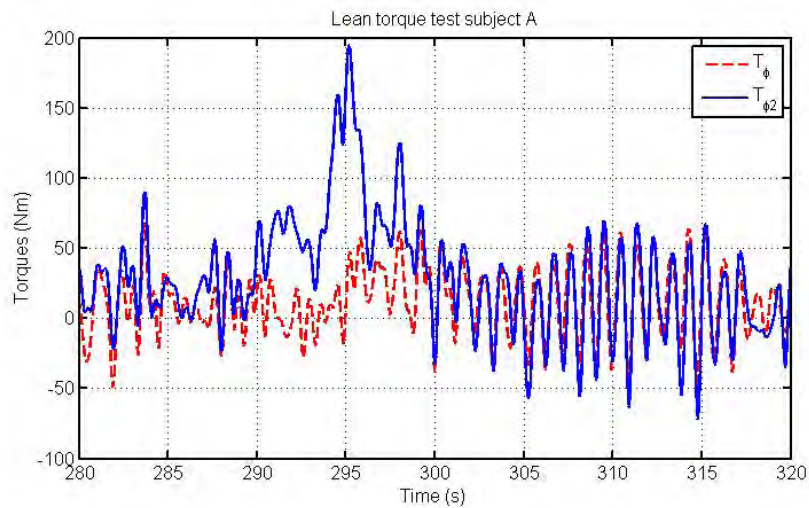
(b) The calculated lean torque, referred to as T_ϕ, along with an estimation of the lean torque, based on the lean angle of the rider, referred to as $T_{\phi2}$

Figure 8.16:

8.7 Frequency content

In order to provide more than only the amplitude of the measured signals the frequency contents of the measured signal of the steering angle, the measured torque and the measured roll angle of the bicycle are shown in figure 8.17(a) and figure 8.17(b).

Small interval

From the figure can be seen that frequencies beyond 2 Hz are hardly present. This is not due to the method of filtering since this effect was already visible in figure 8.2.

The figure shows a small peak at 1 Hz for the torque that was measured by the torque sensor. This is due to the pedalling frequency of the test subject. The rider moves his/her entire body with the pedalling frequency. The rider is thereby applying a small torque to the handlebars by doing this. From figure 8.9(a) can be seen that the average pedalling frequency on the interval 295 sec to 320 sec is near 1 Hz. This small peak is also present in the frequency content of the roll angle. This is because the rider applies a torque to the entire bicycle by moving his/her body. This can be looked as as an harmonic excitation. The torque the rider applies by moving his/her body was explained earlier in section 8.6.

The figure also shows a peak for both the roll angle and the steer angle at 0.27 Hz. The cause for this is unknown, a possibility is that this peak is related to the duration of the curve.

Larger interval

Figure 8.17(b) shows the frequency contents of the steering angle, the measured torque and the measured roll angle of the bicycle. This is shown for the same parameters and the same rider (test subject A) as in figure 8.17(a). The difference however that instead of the relatively small interval of t=280 sec to 320 sec, a larger time interval is chosen. The time interval for this figure is t=280 sec to t=500 sec.

Like figure 8.17(a) this figure shows a peak in the steering torque and the roll angle at a frequency near 1 Hz.

A difference however is that a peak is shown in the steer angle and the roll angle at a frequency of 0.344 Hz which is 2.16 rad/s. A possible cause for an oscillation at that frequency is the weave oscillation which is can be seen in figure 8.1. According to this figure and the average speed of the bicycle (4.63 m/s) in the time interval the frequency of oscillation of the weave motion should be 2.26 rad/s.

The oscillation frequency that occurs at this measurement of 2.16 rad/s is a lower frequency than the oscillation of the weave motion of the dynamic system of the uncontrolled bicycle (2.26 rad/s). This could be caused by the fact that this is not an uncontrolled bicycle. The hands that are connected to the handlebars lower the frequency that occurs. This means that the peak at the frequency of 0.344 Hz could well be caused by the weave oscillation of the dynamic system of the bicycle including the rider.
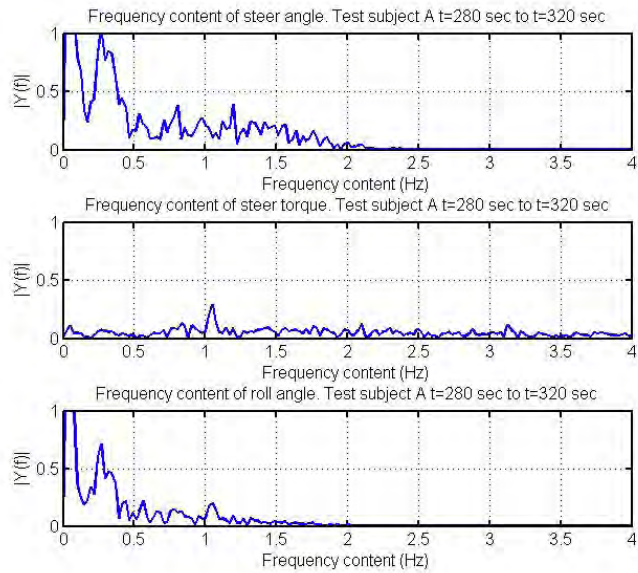
(a) Frequency content of the measured and filtered data of: the steering angle, the torque measured by the torque sensor, the roll angle of the bicycle. This is shown for test subject A on the interval of 280 sec to 320 sec which is shown in figure 8.6(a) in red.
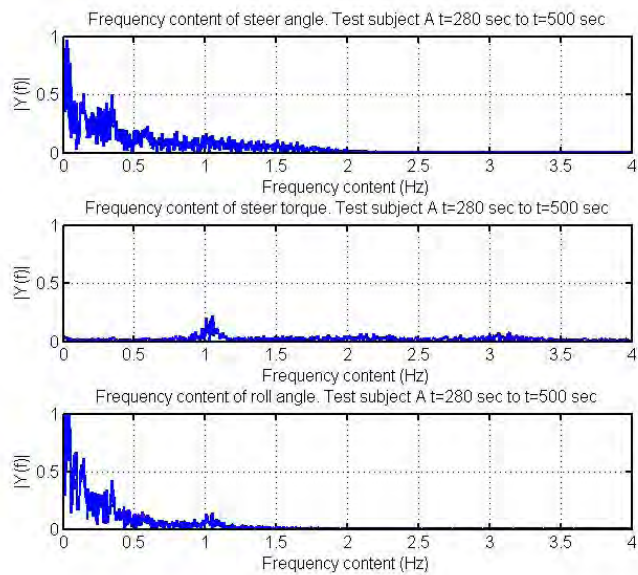
(b)

Figure 8.17:

Chapter 9

Data results

9.1 Range of sensors

Range check

Since the objective of the measurements is to find the maximum values of the different parameters, the range of the different sensors is very important. The sensors have been selected before the amplitude of measured values was known. Therefore it is easily possible that the range of some sensors is exceeded.

Sensor	Range
Accelerometer MTI-g	50 m/s^2
Rate gyroscope MTI-g	5.2 rad/s
Torque sensor	4.98 Nm
Electric motor	8.13 m/s
Potentiometer (steer angle)	45°
Potentiometer (lean angle)	90°
Accelerometer	100 m/s^2

Table 9.1: The range of the different sensors that were used for the measurements

Two of these sensors exceeded their range during the measurements. This was not discovered early because the first few test subjects did not exceed the range of the sensors. The sensors for which the range was exceeded are the following.

- The potentiometer that measures the steering angle.

- The torque sensor that measures the steering torque.

Potentiometer measuring the steering angle

The potentiometer that was used is a linear multi turn potentiometer with a conductive plastic resistance described in section 5.2. The rotation of the potentiometer is unlimited, this means that when the maximum resistance is reached and the potentiometer is rotated further the resistance will change to 0 and start over. This is exactly what happened during the measurements.

The angular velocity of the steer angle showed large spikes at the time instants were the voltage measured by the data acquisition device instantly went from 9 V to 0 V. The signal was reconstructed using the spikes in the angular velocity of the steer angle. In certain intervals the data was shifted to correct the error caused by the limitations.

Torque sensor measuring the steering torque

Problem

As was described in section 5.7 the eventual range for the torque sensor was 3.75 Nm. For short periods of time however overloading of the sensor is possible. This way the maximum torques that were measured were often higher than the maximum torque the torque sensor could officially withstand.

The measured data however was limited by the settings of the amplifier. Since prior to the measurements lower extremes were expected the level of amplification of the amplifier was set accordingly. After the measurements the limitations became clear.

These are the maximal values for all the groups together.

```
-4.9214 Nm
 4.8075 Nm
-4.8852 Nm
 4.0843 Nm
 4.8656 Nm
-3.2717 Nm
-3.8245 Nm
 4.2618 Nm
-4.5216 Nm
-4.9397 Nm
-4.4085 Nm
 4.3378 Nm
-3.7389 Nm
 3.0319 Nm
-4.2577 Nm
-4.5896 Nm
-5.1114 Nm
```

```
 4.4018 Nm
-5.0257 Nm
-4.9806 Nm
```

Many of the values ar near the boundary, the limit is reached. For the extreme values of 4.98 Nm or more and -5.0 Nm or less the voltage reaches +10 V or -10 V which is the limit of the voltage that can be measured by the data acquisition device.

In this section a solution to the insufficient range of the torque sensor will be presented. First of all the density function of the measured torque of a measurement will be investigated. Then based on all the density functions an estimate is made for the extreme values that could have been measured.

Investigation density function

In order to still be able to make an estimate of the steering angle the probability density function was investigated. The probability density based on the measured values for one of the riders is shown in figure 9.1(a).

In the figure can be seen that the distribution is almost symmetrical. The distribution that is most suitable for this purpose is a distribution called the logistic distribution. This distribution can be fitted with the density function shown in figure 9.1(a). The best fit for this distribution is found using Matlab.

```
mu = 0.000961619
sigma = 0.325019
```

The probability density function of this distribution along with the density distribution is shown in figure 9.1(b).

For this particular rider the extreme value is the following.

```
-4.5216 Nm
```

The cumulative distribution function can be used in order to find out what the probability is (for each point of measurement) for finding a value smaller or equal to the value that was measured. The probability of measuring this value or a value that is even smaller is the following.

```
0.0015 %
```

Making an estimate for the extreme values

Using the method in the previous paragraph the probability of measuring the extreme value can be calculated for each measurement in which the torque stays well within the limitation of the sensors. Although one rider uses more more torque than a different rider the thing that is changed by this is not the probability of measuring the extreme value. The thing that changes with the amount
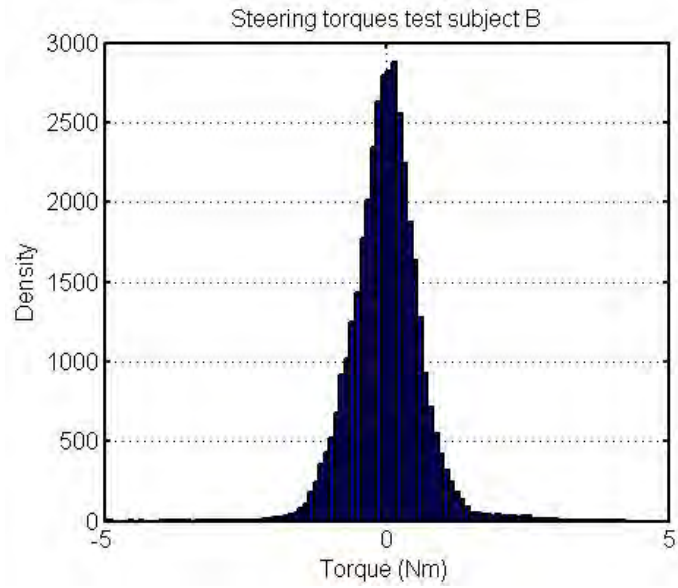
(a) Density of the steering torque of a rider while riding the bicycle (speed is larger than 0.5 m/s)
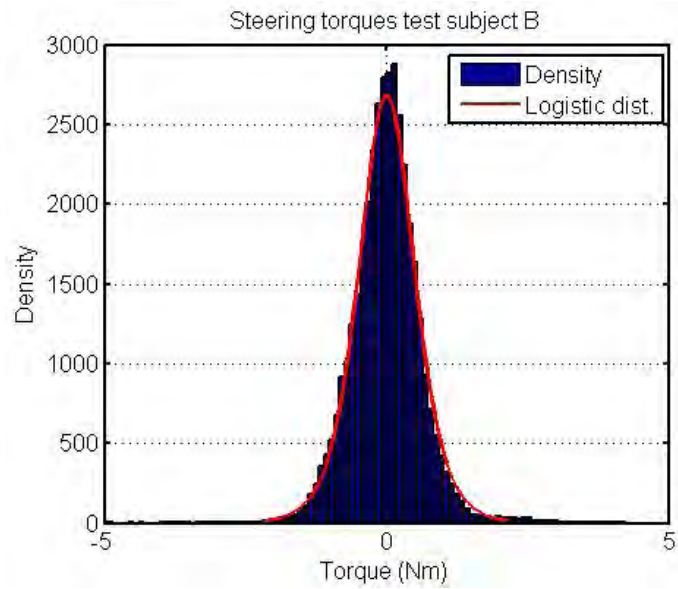
(b) The logistic distribution fitted with the density distribution of the steer torques

Figure 9.1:

of torque a rider uses is the standard deviation and therefore the corresponding probability density function that is fitted with the torques that were measured during the measurement. The probability of measuring the extreme value should in theory be the same for every rider.

The average value of the probabilities of measuring the extreme value is the following.

```
0.0032 %
```

The next step is to apply this method inversely on the measured data using the mean value of the probabilities (0.0032 %). The result is an extreme value for each measurement based on the density distribution of the measurement. The resulting extreme values that are now found are the following.

```
4.9933 Nm
3.9402 Nm
4.4772 Nm
3.4952 Nm
5.3451 Nm
4.0307 Nm
4.1599 Nm
3.5982 Nm
4.6156 Nm
3.7017 Nm
4.1170 Nm
5.3484 Nm
3.4689 Nm
3.8067 Nm
4.1450 Nm
3.8726 Nm
4.3853 Nm
4.0786 Nm
4.2440 Nm
4.6662 Nm
```

Note that for convenience the values were changed to absolute value. This makes no difference for the result because the absolute value of the extreme values is the only thing that is considered in the analysis explained in section 6.2. Also note that for all the measurements the extreme value has changed only parameter that influences the extreme value is now the standard deviation of the measured values. The standard deviation is now the only random factor.

9.2 Extreme value and estimated extreme value

In section 6.2 the method of determining the range in which the mean value of the maximum values for certain parameters can be found. Figure 9.2(a) shows the distribution of the maxima of the centripetal acceleration for the group of average riders. In this figure the range in which the mean value can be found is also shown. This mean lies between 3.4558 m/s^2 and 3.8242 m/s^2.

> Of what value is the range for the mean of the maxima of parameters? Wouldn't the total maximum be more helpful for a design?

In this section this question will be answered. For this example of the centripetal acceleration the total maximum can give the maximum measured value for the group of test subjects. If the same measurement would be repeated infinitely many times for an infinite group of test subjects the total maximum would always be higher than the total maximum of this group of 12 test subjects. The question is: in what range would that total maximum be?

The range for the mean value of the maxima when an a large amount of test subject would be measured can be found using the bootstrap principle explained in section 6.2. A way of estimating the maximum of the dataset when measuring a large amount of test subject is by shifting the currently found distribution until the mean of the distribution is at the maximum of the range for the mean. In this case the mean value of the shifted distribution should become 3.8242 m/s^2. The shifted distribution along with the original distribution is shown in figure 9.2(b).

The estimate of the maximum value when measuring a large amount of test subjects is now the maximum value in the shifted distribution. Which is 4.4238 m/s^2. Please note that this is just an estimate of the maximum, there is no proof that none of the test subjects would ever exceed this estimate value. However the number of test subjects exceeding this estimate of the maximum will be small relative to the total number of test subjects.
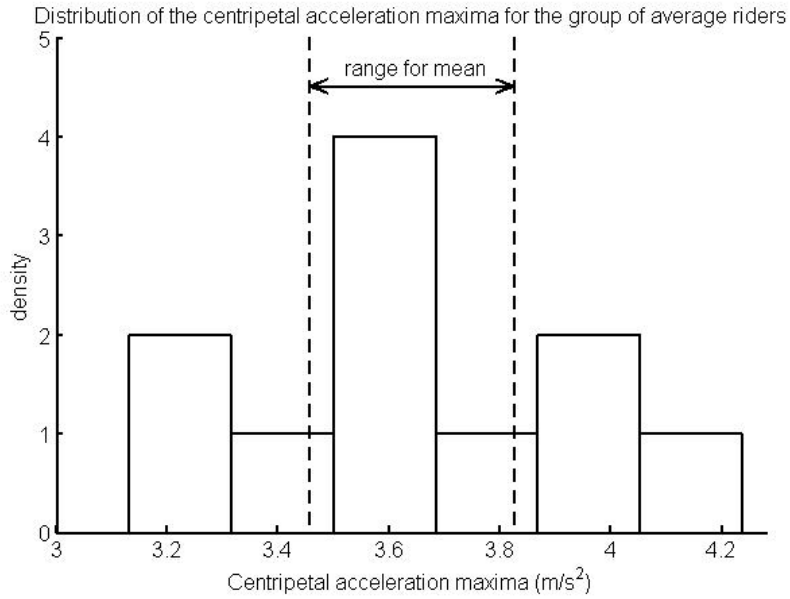
(a) The distribution of the maxima of the centripetal acceleration. The range in which the mean value will be found when measuring a large quantity of test subjects is shown as well.
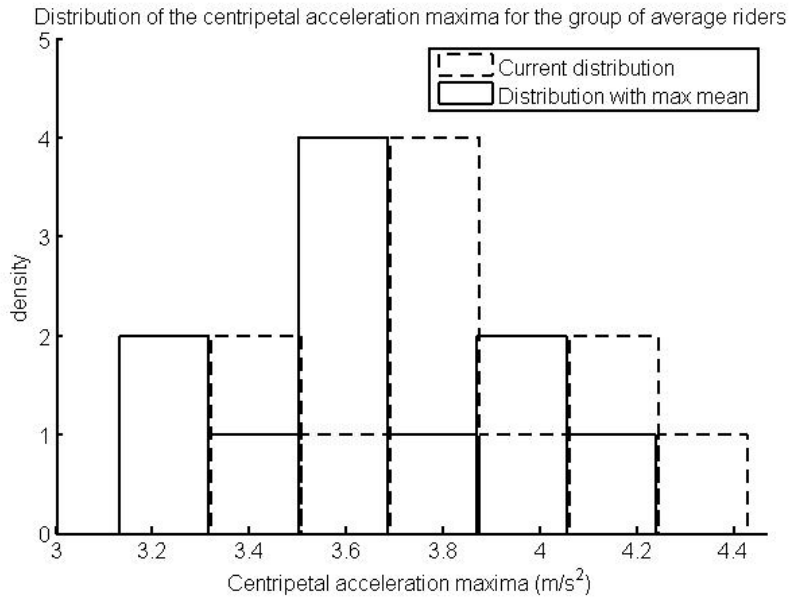
(b) The distribution of the maxima of the centripetal acceleration along with a shifted distribution, the shifted has the maximum possible mean value.

Figure 9.2:

9.3 Distribution results

In figure 9.1(a) the density distribution of the measured torques were shown for for an arbitrary rider. The standard deviation along with the mean value tells much a about a distribution. In order to provide some information about the distribution of the measured values, the following values are shown for each parameter.

- mean of all the mean values of the measurements.

- mean of all the standard deviations of the measurements.

This is done for each of the three different groups of test subjects. The results are shown below. Note that this has nothing to do about the extreme values of the measurements.

Group	Average		Elderly people		Inexperienced	
Parameter	mean	std	mean	std	mean	std
forward acc. (m/s^2)	0.14	0.30	0.14	0.31	0.15	0.24
roll angle (degrees)	0.02	3.05	0.03	2.63	0.03	2.15
roll speed (rad/s)	0.00	0.09	0.00	0.08	0.00	0.07
roll acc. (rad/s^2)	-0.00	0.46	-0.00	0.42	0.00	0.34
roll jerk (rad/s^3)	-0.00	3.04	-0.00	2.84	-0.00	2.24
yaw speed (rad/s)	0.05	0.18	0.05	0.16	0.04	0.17
yaw acc. (rad/s^2)	-0.00	0.71	0.00	0.68	-0.00	0.67
steer angle (degrees)	0.14	4.78	0.15	4.35	0.08	5.98
steer speed (rad/s)	0.00	0.25	0.00	0.24	0.00	0.34
steer torque (Nm)	0.00	0.70	-0.00	0.69	0.01	0.78
centripetal acc. (m/s^2)	0.21	0.66	0.21	0.58	0.11	0.42

Table 9.2: Table showing the (mean) mean and the (mean)standard deviation of the different measurements. Note that this has nothing to do with the extreme values.

Figure 9.4 shows information about the distribution of the series of the extreme values of the different measurements.

9.4 Extreme values results

The method that was discussed in 6.2 was applied to the data from all the measurements. For the parameters of which the sensor range was insufficient (discussed in section 9.1) was corrected using the methods discussed in section 9.1 and section 9.1. This way a range for the mean is found for each of the parameters determined in chapter 4.

Next the estimated maximum was calculated from the range for the mean value

and the current maximum value. This method is explained in section 9.2.

The results from these calculations for the three groups of test subjects, average riders, elderly people and inexperienced riders are shown in the rest of this section.

Average riders

Parameter	Range for mean	Mean	Max.	Est. Max.	No.
forward acc. (m/s^2)	1.65 ± 9.89 %	1.65	2.06	2.22	11
roll angle (degrees)	17.17 ± 5.66 %	17.31	19.22	20.05	11
roll speed (rad/s)	0.40 ± 10.49 %	0.39	0.51	0.56	11
roll acc. (rad/s^2)	1.89 ± 12.80 %	1.92	2.34	2.54	11
roll jerk (rad/s^3)	12.77 ± 11.70 %	12.95	16.38	17.69	11
yaw speed (rad/s)	1.05 ± 6.46 %	1.06	1.21	1.27	11
yaw acc. (rad/s^2)	3.19 ± 12.39 %	3.18	4.55	4.96	11
steer angle (degrees)	51.13 ± 13.20 %	50.55	75.85	83.17	12
steer speed (rad/s)	2.33 ± 15.27 %	2.31	3.35	3.72	12
steer torque (Nm)	4.28 ± 8.46 %	4.24	5.35	5.75	10
centripetal acc. (m/s^2)	3.64 ± 5.05 %	3.63	4.23	4.43	11

Table 9.3: For the group of average riders; the range in which the mean of the extreme values can be found. The mean of the extreme values is also shown as well as the current maximum and the estimated maximum. The last collum shows the number of measurements that contained usable data that was used to calculate this result.

From table 9.4 can be seen what the results are of the calculations that were done. The parameter that is most important for the design of the simulator is the estimated maximum value. This value should provide an estimate for the maximum value for the corresponding parameter that will not be exceeded by any rider.

One thing that is notable is that these estimated maximum values are lower than for the other groups except for one parameter, the steer angle. The current maximum value of the steer angle is 75.85°. The estimated maximum value due to the range for the mean value is consequently 83.17°. These steer angles that were measured were larger than expected. The largest steer angle during a measurement occurs in all the cases during a start or a stop.

The cause for this group of riders reaching a larger steer angle is yet unknown. A likely cause of this effect is that this group is the least careful group. Elderly people are more careful to prevent themselves from falling because falling imposes a greater risk of injuries for them. The inexperienced riders are also

careful to prevent themselves from falling because the likelihood of a fall is larger for people in this group.

Elderly people

Parameter	Range for mean	Mean	Max.	Est. Max.	No.
forward acc. (m/s^2)	1.67 ± 6.14 %	1.69	1.88	1.97	8
roll angle (degrees)	16.28 ± 15.53 %	15.83	22.03	25.02	8
roll speed (rad/s)	0.45 ± 11.29 %	0.45	0.55	0.60	7
roll acc. (rad/s^2)	1.98 ± 10.73 %	1.98	2.44	2.65	7
roll jerk (rad/s^3)	13.14 ± 12.35 %	13.05	16.12	17.84	7
yaw speed (rad/s)	1.06 ± 6.60 %	1.06	1.22	1.30	7
yaw acc. (rad/s^2)	3.79 ± 12.00 %	3.61	4.84	5.47	7
steer angle (degrees)	43.30 ± 13.15 %	42.88	58.87	64.99	9
steer speed (rad/s)	2.57 ± 17.11 %	2.54	3.92	4.39	9
steer torque (Nm)	4.27 ± 9.06 %	4.15	5.35	5.86	8
centripetal acc. (m/s^2)	3.63 ± 14.91 %	3.56	4.74	5.35	7

Table 9.4: For the group of elderly people; the range in which the mean of the extreme values can be found. The mean of the extreme values is also shown as well as the current maximum and the estimated maximum. The last collum shows the number of measurements that contained usable data that was used to calculate this result.

From table 9.4 can be seen what the results are of the calculations that were done. The parameter that is most important for the design of the simulator is the estimated maximum value. This value should provide an estimate for the maximum value for the corresponding parameter that will not be exceeded by any rider.

One thing that is notable is that maximum value of the roll angle and centripetal acceleration are for this group larger than for the other groups even though the mean value is lower. For each measurement the maximum value of these two parameters occur in a curve. This was again an unexpected result. Apparently some of the measured elderly people do not decrease their speed when approaching a curve as much as normal riders and inexperienced riders. The cause for this effect is yet unknown.

Something else that is notable is that the current maximum value of the steer speed is larger for this group than for the group is average riders. This maximum occurs normally during a start or during a stop. Apparently, where average riders simply use a large steer angle, elder people use a quick change of the steer angle to stabilize the bicycle.

Unexperienced riders

Parameter	Range for mean	Mean	Max.	Est. Max.	No.
forward acc. (m/s^2)	1.60 ± 29.44 %	1.60	2.07	2.54	2
roll angle (degrees)	14.28 ± 24.32 %	14.28	17.75	21.23	2
roll speed (rad/s)	0.39 ± 21.47 %	0.39	0.48	0.56	2
roll acc. (rad/s^2)	1.74 ± 10.97 %	1.74	1.93	2.12	2
roll jerk (rad/s^3)	13.52 ± 14.45 %	13.52	15.47	17.42	2
yaw speed (rad/s)	0.84 ± 3.34 %	0.84	0.87	0.90	2
yaw acc. (rad/s^2)	4.20 ± 7.34 %	4.20	4.51	4.82	2
steer angle (degrees)	47.21 ± 4.17 %	47.21	49.18	51.15	2
steer speed (rad/s)	3.87 ± 3.37 %	3.87	4.00	4.13	2
steer torque (Nm)	4.46 ± 4.74 %	4.46	4.67	4.88	2
centripetal acc. (m/s^2)	1.97 ± 10.48 %	1.97	2.18	2.39	2

Table 9.5: For the group of unexperienced riders; the range in which the mean of the extreme values can be found. The mean of the extreme values is also shown as well as the current maximum and the estimated maximum. The last collum shows the number of measurements that contained usable data that was used to calculate this result.

From table 9.4 can be seen what the results are of the calculations that were done. The parameter that is most important for the design of the simulator is the estimated maximum value. This value should provide an estimate for the maximum value for the corresponding parameter that will not be exceeded by any rider.

One thing that is notable is that the current maximum value of the angular velocity of the steer angle is large for this group compared with the other groups. This maximum occurs again during the start for both the measurements. Apparently, where average riders simply use a large steer angle, inexperienced riders use a quick change of the steer angle to stabilize the bicycle.

Something else that is notable is that the maximum value of the yaw speed is small for this group compared with other groups. This is due to a reduced velocity of these rider throughout the entire track. Apparently reducing their velocity feels safer for them despite the fact that a bicycle is instable in the lower speed range.

Figure 9.3: bump

9.5 Overview

Figure 9.4 shows an overview of the extreme values that were measured during the measurements. The extreme value of all riders is shown per group and per variable. While viewing this figure one should keep in mind that the data of the inexperienced riders consists of only two measurements. In this figure that is two data points. The median, upper and lower quarter and outliers cannot be shown calculated based on two data points and therefore they cannot be shown in the figure.
The most striking differences are discussed in this section. The smaller differences are ignored.

As was discussed earlier the maximum roll angle and the maximum centripetal acceleration is larger for the group of elderly people. The mean however for this group is lower than the mean for the group of average riders. Apparently some of the measured elderly people do not decrease their speed while approaching a curve as much as average riders would do. The cause for this is yet unknown.

Another striking insight this figure gives is that the group of elderly people as well as the group of inexperienced riders in average did not rotate the handlebars as far as the group of average riders. This could indicate that that this group of average riders is less careful that the other groups and has more confidence.

The roll rate shows that the maximum value of the roll rate of the group of elderly people is larger than for the other groups. The roll rate is the angular velocity of the bicycle in the roll direction. For the measurements of which the maximum of the roll rate is relatively large compared to the maxima of the other riders these maxima occurred at the same location in the route. Namely at a speed bump the location of this maximum riders that showed this large maximum value. The speed bump is situated in such a way that a cyclist practically needs to be changing direction at the very moment he/she start to go over this bump. At this moment the maximum roll rate occurs for these riders.
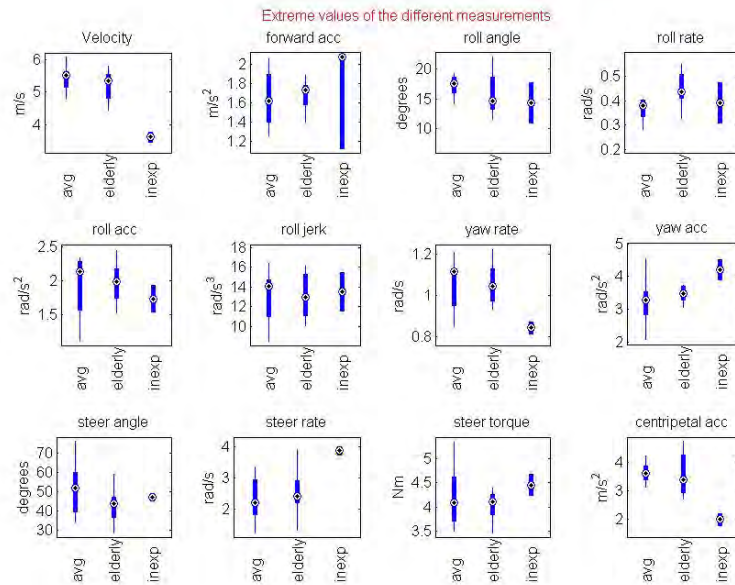
91

Figure 9.4: The extreme values of all test subjects shown in boxplots

The speed bump is shown in figure 9.3.

Furthermore the extreme values from the inexperienced rider show a strikingly different range of extreme values for the following parameters: velocity, yaw rate, yaw acceleration, steer rate, steer torque, centripetal acceleration.
The velocity of the group of inexperienced riders is lower than both other groups. This is characteristic for international students that are inexperienced cyclists. The cause of this is yet unknown. Most likely this relatively low velocity is related with fear of falling. This relatively low velocity has as a result that (since the velocity in the curves is also relatively low) the yaw rate maxima and centripetal accelerations are low.
The higher angular velocity of the steer rate, the higher angular accelerations of the yaw angle and the higher steer torques are probably related with the low velocity of the bicycle. Since the rider is driving the bicycle at a low velocity more control is required in order to keep the bicycle upright.

Chapter 10

Conclusion

In section 9.4 the results were shown for the different groups. As was mentioned before the estimated maximum is the most important value for the design of a bicycle simulator. Since all three groups of people should be able to rider the bicycle simulator, the largest estimated maximum is the chosen as the maximum for the recommended range.

The largest estimated maximums were used in order to formulate a recommended range for a bicycle simulator. They are shown below in table 10.

Notable is that most of these values were extracted from table 9.4 which shows results for the group of elderly people. This is partly caused by the fact that for three of the parameters the largest maximum values were found in this group of test subject. A second cause for this is that fewer measurements were done with test subjects from this group, this has as a result that the range for the mean of the maximum is larger and consequently the estimated maximum becomes larger.

Parameter	Recommended range
forward acc.	$[0\ m/s^2,\ 2.22\ m/s^2]$
roll angle	$\pm 25.02°$
roll speed	± 0.6 rad/s
roll acc.	$\pm 2.65\ rad/s^2$
roll jerk	$\pm 17.84\ rad/s^3$
yaw speed	± 1.3 rad/s
yaw acc.	$\pm 5.47\ (rad/s^2)$
steer angle	$\pm 83.17°$
steer speed	± 4.39 rad/s
steer torque (Nm)	± 5.86 Nm
centripetal acc.	$\pm 5.35\ m/s^2$

Table 10.1: The recommended range for the different parameters for the design of a bicycle simulator

When a designer applies this recommended range to his design of a bicycle simulator he will apply a safety factor to this range in order to be on the safe side. The maximum forward acceleration range for example of $[0\ m/s^2,\ 2.22\ m/s^2]$ could be rounder off to $[0\ m/s^2,\ 2.5\ m/s^2]$. This safety factor has not yet been applied to the data in this report in order to give the designer the opportunity to choose his own safety factor.

The frequency range that is found for all these parameters is similar to that of figure 8.17(b). This means frequencies beyond 2 Hz are negligible.

Chapter 11

Recommendations

11.1 How to proceed

First step
Now that the required range for the different parameters is known the next step is to devise a working principle for the simulator. The motorcycle simulator described in section 3.1 can serve as an example. The paper [7] named "Objective and subjective evaluation of an advanced motorcycle riding simulator" written by V. Cossalter, R. Lot and S. Rota describes this simulator. Additional information about this simulator is not superfluous. One thing that is mentioned in the paper and which is essential for the construction of the simulator is the use of a "washout filter". The purpose of this washout filter is to recreate the experience of riding the motorcycle with the accelerations as they are present in real life by applying accelerations and the angular velocity of the simulator and the acceleration of gravity. Before constructing a bicycle simulator this type of filter should be investigated.

Second step

In a second step actuators can be selected for the different motions and a controller needs to designed for those actuators. After that an experimental setup can finally be built. Since a graphical interface will be required for a working prototype a possibility is using the interface that from the simulator described in appendix A. Such a prototype of the simulator provides insight in how to proceed. Deficiencies in the design will then be revealed. An important test for this prototype would also be to have inexperienced cyclists ride the prototype of the simulator. This is also much safer than actual measurements on a bicycle.

Third step

A third step is to create a intuitive graphical interface. If the control of the

simulator is done using Matlab the graphical interface could be constructed using the virtual reality toolbox in Matlab together with 3D Max. The view of the simulator is also important. The motorcycle simulator discussed earlier has a first person interface, this means that the view of the interface is through the eyes of the rider on the motorcycle. Third person is also a commonly used view, this is a view where the rider on the bicycle is seen from the back. In the gaming industry it is customary to provide both and provide the possibility to the user to select his/her personal preference.

Fourth step

The fourth step is to develop a consumer product. The experimental setup serves as a starting point. Since the experimental setup is probably a relatively large construction the consumer product needs to be more compact and easy to use. The development of the simulator is best done in cooperation with companies such as for example Tacx. Tacx could provide useful data such as force a rider applies to the pedals and friction in bicycles.

11.2   Future measurements

Replace bicycle

Something that was noticed during measurements with international PhD students is that the bicycle that is used for measurements is too large and that is difficult for women to get on it.

A different bicycle should be acquired for future measurement that is easily adjustable for people of all sizes. A folding bicycle would be a good pick since folding bicycles are small and easily adjustable. The only drawback is that de dynamics of such a bicycle are different.

Potentiometer

When analyzing the measurement the following was noticed. The range of the potentiometer measuring the steer angle was exceeded. This is was described in section 9.1. Test subjects exceeded the range of the steer angle that can be measured by the potentiometer (-45° to 45°). Either the potentiometer should be replaced or a different toothed pulley should be installed on the potentiometer realizing a different transfer ratio. For details about the instrumentation for measurement of the steer angle see section 5.2.

Rider lean

During measurements the tube connecting the potentiometer with the backpack proved to be inconvenient for the rider. Also the hinge that is located near

the backpack showed vibrations which is unwanted. After every stop there was also an offset in the measured angle as if the backpack or the rider had moved left or right. Eventually the measurements of the rider lean were not used because the measurements were unreliable. For future measurement a possibility is using a IR sensor along with two IR-transmitters. The transmitters could be connected for example to the shoulders of the rider. This system of measuring the location of an object is also used in a Nintendo Wii gaming console.

Design torque sensor

The range of the torque sensor was insufficient to measure the maximum torque for every rider. This was described in section 9.1. A more convenient way of designing the torque sensor would have been by using one load sensor instead of two. The range of the torque sensor should at least be 6 Nm. A better functioning overload protection is recommended, a possibility is using a slip clutch.

When a design with a torque sensor instead of load sensors would be created the following web site could provide useful information.
http://biosport.ucdavis.edu/research-projects/bicycle/instrumented-bicycle/steer-torque-measurement This torque sensor was constructed by Jason Moore one of the authors of the paper [2] named "A method for estimating physical properties of a combined bicycle and rider" that was mentioned before.
A second design is provided in a paper [11] named "Comparison of a Bicycle Steady-State Turning Model to Experimental Data" written by S. M. Cain and N. C. Perkins.

Appendix A

A desktop bicycle simulator

A.1   Introduction

Simulators are often complicated machines which try to offer the complete motion that is involved with the corresponding way of transportation. For most simulators however the gaming industry has created a version that demands less hardware than a real simulator. For example, motor racing games have been developed for the iPad or the computer. They do not apply any motion to the user however unto some extend they can give the user the idea that he/she is riding a motorcycle.

For the purpose of finding out if such a simulator can be created for a bicycle, a desktop version of a bicycle simulator was developed in Matlab making use of only a notebook an a force-feedback steering wheel console. The two main skills that the user should learn while using this simulator:
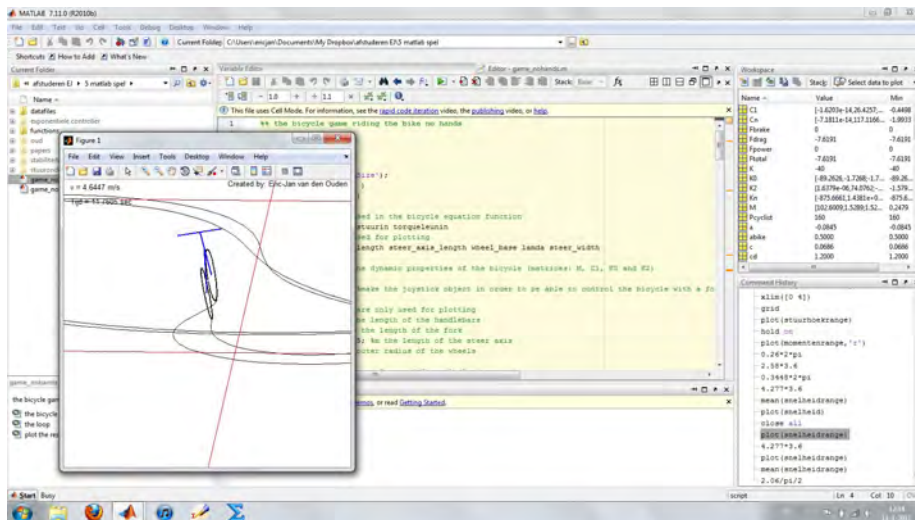
- How to steer in order to prevent yourself from falling

- Going too slow makes it more difficult to prevent yourself from falling

These two skills are essential in the process of learning to ride a bicycle.

Figure A.1(a) shows a picture of the simulator being used by a colleague.

(a) The simulator being used by a colleague

(b) The output shown on the screen in the picture in figure A.1(a)

Figure A.1:

A.2 Model

Relations

An example of a bicycle simulator was constructed using an existing dynamic model of a bicycle with rider. The model used is mentioned in an article written by J.P. Meijaard [1]. Parameters of the bicycle that was simulated are mentioned in a conference paper written by A.L. Schwab [3], the name of the paper is: "Linearized dynamics equations for the balance and steer of a bicycle: a benchmark and review". This model is also commonly referred to as: "The benchmark bicycle".

The coordinate system of the model is shown in figure 3.3.

The differential equation that governs the movement of the bicycle mentioned in section 3.2. This is equation 3.1.

$$M\ddot{q} + vC_1\dot{q} + [gK_0 + v^2K_2]q = f$$

In which $q = [\phi; \delta]$ which are respectively the lean angle and the steer angle, $f = [T_\phi; T_\delta]$ which are respectively, the torque caused by lateral movement of the rider and the steering torque.

The matrices M, C_1, K_0 and K_2 are known for this bicycle. They are mentioned in the a paper written by Jason Moore [2].

$$M = \begin{pmatrix} 102.6009 & 1.5289 \\ 1.5289 & 0.2479 \end{pmatrix} C_1 = \begin{pmatrix} -0.0000 & 26.4257 \\ -0.4498 & 1.0271 \end{pmatrix}$$

$$K_0 = \begin{pmatrix} -89.2626 & -1.7268 \\ -1.7268 & -0.6719 \end{pmatrix} K_2 = \begin{pmatrix} 0.0000 & 74.0762 \\ -0.0000 & 1.5579 \end{pmatrix}$$

In order to reduce this from a second order to first order differential equation the model is expanded into:

$$\begin{bmatrix} \ddot{\phi} \\ \ddot{\delta} \end{bmatrix} = M^{-1} \begin{bmatrix} - & vC_1 & -K_0g - v^2K_2 \end{bmatrix} \begin{bmatrix} \dot{\phi} \\ \dot{\delta} \\ \phi \\ \delta \end{bmatrix} + f$$

$$\begin{bmatrix} \dot{\phi} \\ \dot{\delta} \end{bmatrix} = \begin{bmatrix} 1 & 0 & 0 & 0 \\ 0 & 1 & 0 & 0 \end{bmatrix} \begin{bmatrix} \dot{\phi} \\ \dot{\delta} \\ \phi \\ \delta \end{bmatrix}$$

With the following substitution the relation is put into a form that can be integrated using an ordinary differential equation solver in Matlab.

$$y = \begin{bmatrix} \dot{\phi} \\ \dot{\delta} \\ \phi \\ \delta \end{bmatrix}$$

The differential equation has now been put into the form:

$$\dot{y} = Ay + f$$

Next, since ϕ, δ and v are known the heading and the position of the bicycle can be found. This is done in the same way as described in section 3.2.

Also the speed of the bicycle will be a changing variable. In order calculate the forward speed the sum of the forces is found in the following way.

$$\sum F_{forward} = \frac{P_{rider}}{v} - F_{brake} - F_{drag} \tag{A.1}$$

With P_{rider} being the power the rider applies to the pedals, F_{brake} is the effect of the brakes represented in the form of a force from the ground to both the tires of the bicycle. F_{drag} is the force caused by air drag. The value of P_{rider} and F_{brake} is discussed in section A.3.

The force applied by air drag on the bicycle and rider is governed by the following relation.

$$F_{drag} = \frac{1}{2}C_D \cdot A_F \cdot \rho \cdot v^2 \tag{A.2}$$

The values for the different parameters in the above equation are shown in table A.2.

The bicycle accelerates according the sum of the forces calculated by equation A.1 in the following way.

$$\sum F_{forward} = m_{total} \cdot a_{forward} \tag{A.3}$$

Parameters

Several parameters were used for simulating with the model. Table A.1 shows the parameters that were used, all the parameters that were used have been extracted from the paper written by A.L. Schwab [3] that was mentioned earlier.

Parameters that are related with drag are taken from a book written by D.G. Wilson called 'Bicycling Science'[4]. These parameters are shown in table A.2.

Table A.1: Parameters of the bicycle used in the model.

Parameter	Symbol	Value
Wheel base	w	1.121 m
Trail	c	0.0686 m
Steer axis tilt	λ	22.9°
Gravity	g	9.81 m/s^2
Forward speed	v	various m/s
Mass bicycle and rider	m_{total}	95.5 kg

Table A.2: Parameters related to drag

Parameter	Symbol	Value
Drag coefficient	C_D	1.2
Frontal surface area of a regular bicycle and rider together	A_F	0.5 m^2
Density of air at sea level	ρ	1.293 kg/m^3

Figure A.2: The force-feedback steering wheel that was used for the input and the feedback of the model

A.3   Input and feedback

Hardware

The steering wheel that was used in order to provide input for the model and feedback from the model to the user by applying a torque is shown in figure A.2. As can be seen in the picture the steering wheel also has two pedals on the floor which can be used for accelerating and braking.

Interfacing with the steering wheel is possible in Matlab. Using a command and some calculations the angle of the steering wheel can be measured. Using a different command it is even possible to apply a torque on the steering wheel.

The steering wheel cannot however measure the torque that is applied to it of angular acceleration or velocity.

Interface

The interface of the simulator is shown in figure A.3. This interface has been carefully constructed. The bicycle rotates about its roll axis. The steering assembly rotates about the steering axis. Even the wheels of the bicycle rotate according to the speed of the bicycle.

The bicycle in the interface is not moving forward nor changing heading however, the grid lines are moving and rotating according with the speed and the yaw angle of the bicycle. The tracks from the wheels of the bike are even shown. The viewing area along with the spacing of the grid lines and the viewing area have been selected by trial and error.
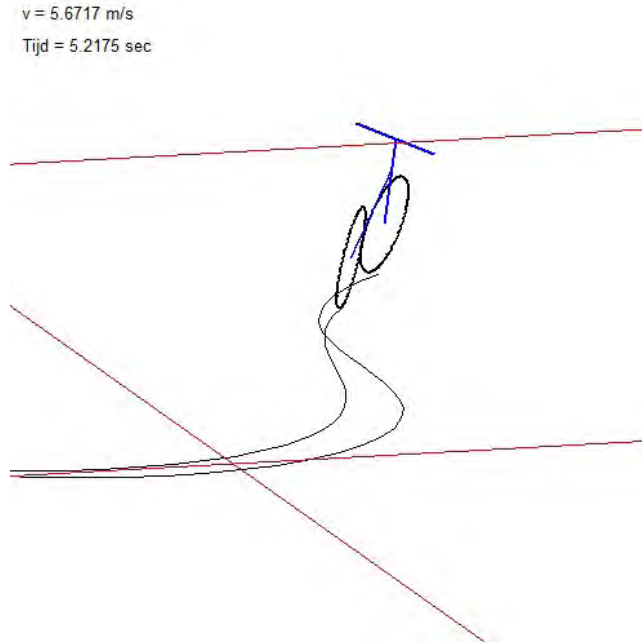
Figure A.3: The interface that is shown during the simulation

Program

The rider is able to change the speed of the bicycle using the two pedals shown in figure A.2. The right pedal is used in order to apply power to the bicycle. The power applied to the bicycle is governed by the following relation.

$$P_{rider} = f_{rightpedal} \cdot 160 \tag{A.4}$$

In which $f_{rightpedal}$ is the fraction indicating how far the right pedal is pressed on a scale of 0 to 1.

The left pedal is used for braking.

$$F_{brake} = f_{rightpedal} \cdot 60 \tag{A.5}$$

In which $f_{leftpedal}$ is the fraction indicating how far the right pedal is pressed on a scale of 0 to 1.

Torque based input

In an ideal situation the input torque could be measured by the steering wheel which can then be applied on the bicycle model. The force feedback of the steering wheel could then be used in order to make the steering wheel feel exactly like the handlebars of the bicycle.

The torque that the rider of a normal bicycle feels in the handlebars.

$$T_{bicycle} = -M_{\delta\phi}\ddot{\phi} - vC_{1\delta\delta}\dot{\delta} - vC_{1\delta\phi}\dot{\phi} - g\left[K_{0\delta\delta}\delta + K_{0\delta\phi}\phi\right] - v^2\left[K_{0\delta\delta}\delta + K_{0\delta\phi}\phi\right]$$
(A.6)

The inertia of the steering wheel however is different from the inertia of the steering assembly of a bicycle. The torque that should be applied to the steering wheel in order to make it feel like the handlebars of a bicycle.

$$T_{out} = T_{bicycle} + I_s\ddot{\delta}$$
(A.7)

In which I_s is the inertia of the steering wheel about its axis of rotation.

However the force-feedback steering wheel that is used cannot measure any angular acceleration. The only output is the angle of the steering wheel. The angular acceleration could then be found by differentiating the angle twice. Then the euler equation can be used in order to find the sum of the torques that was applied to the steering wheel

$$\sum T = I\ddot{\delta}$$
(A.8)

Sadly enough practice proved that this input method did not work properly. The cause for this is that by differentiating twice a delay was incorporated in the input to the model. This causes problems, since the input had a delay, the resulting T_{out} that came out of the model was not accurate. A growing difference between the steering angle in the model and the steering angle at the steering wheel existed in this version of the program.

The response force feedback torque will always be too late to make the angle of the steering wheel correspond with the angle of the handlebars in the model.

Rotation based input of steer angle proportional controller

A convenient method of controlling the bicycle would be if the angle of the steering wheel would always be equal to the angle of the handlebars of the bicycle in the model.

In an attempt to achieve this the following method of input was constructed.

$$E = \delta_{desired} - \delta$$
$$T_\delta = K_{p1} \cdot E$$
(A.9)

In which $\delta_{desired}$ is the desired steering angle, this is the angle of the steering wheel. K_{p1} is a gain factor that converts the Error E to a torque.
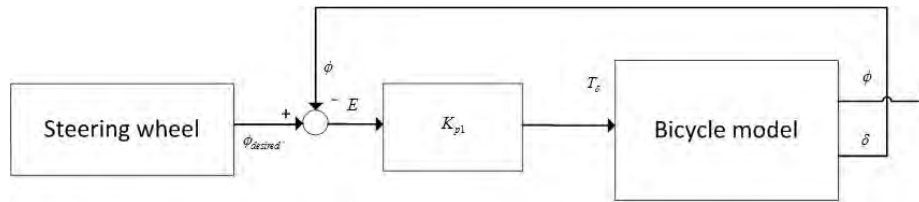
Figure A.4: A flowchart which shows how the Proportional controller for the simulator works. The block shown as "bicycle model" contains no more than equation 3.1

This method of input is illustrated in figure A.4 using a flowchart.

An analogy of this system can be thought of as riding a bicycle with a radial spring connecting the handlebars to the lower stem. Applying torque to the right which can be achieved by turning the steering wheel right has the following effect. The front wheel of the bicycle initially turns right however right after that the bicycle starts leaning left as a result and the front wheel turns left as well even though the rider is still applying torque to the right.

The value of K_{p1} was chosen experimentally. First, since the result of applying torque to the right was making a left turn, negative values of K_{p1} are considered. Because K_{p1} affects the dynamics of the system the stability of the bicycle changed with the value of K_{p1}. A large negative value of K_{p1} made the system unstable at all speeds. A low value of K_{p1} made the effect of the steering wheel small. A convenient value for K_{p1} for which the system was still stable enough turned out to be K_{p1}=-2.

The result was a working version of the desktop simulator. A drawback the steering angle of the steering wheel is not equal to the steering angle of the handlebars in the model. This has as a result that the bicycle cannot be stabilized by the rider at lower speeds. Below 5 m/s it is impossible to keep the bicycle upright.

Also when the bicycle has a roll angle to the right the natural response is to steer to the right in order to stabilize the bicycle. This effect is no longer present in this model. In this model steering to the left stabilizes the bicycle.

This version of input is in the final version of the program however. The Matlab file corresponding with this method of input is named: **game_radialspring.m**.
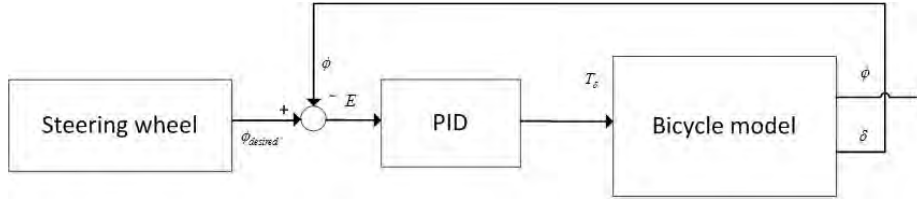
Figure A.5: The steer angle controlled by a PID-controller applying torque.

Rotation based input of steer angle PID-controller

Since proportional control lacked the ability to make the steer angle equal to the desired steer angle a natural next step was applying a PID-controller that makes both these angles equal by applying torque. The torque is now found using the following relation.

$$
\begin{aligned}
E &= \delta_{desired} - \delta \\
T_\delta &= K_r \left(E + \frac{\int E dt}{T_i} + T_d \cdot \frac{dE}{dt} \right)
\end{aligned}
\tag{A.10}
$$

In which $\delta_{desired}$ is the desired steering angle, this is the angle of the steering wheel. This method of input is shown in figure A.5 in a flowchart. The constants K_r, T_i and T_d are chosen experimentally.

This attempt was a failure however, the system was unstable at all speeds. Even after several days of optimizing.

Rotation based input of lean angle proportional controller

In an attempt to create an improved method of input the lean angle of the bicycle was used for control of the applied torque. This approach is based on the idea that the torques that the rider applies is meant to keep the bicycle upright. Path following is not incorporated in this simulator.

In this approach the angle from the steering wheel is the so-called desired roll angle, $\theta_{desired}$. In order to apply a torque that keeps the bicycle upright a proportional controller is used.

$$
\begin{aligned}
E &= \phi_{desired} - \phi \\
T_\phi &= K_{p2} \cdot E
\end{aligned}
\tag{A.11}
$$

In which $\phi_{desired}$ is the desired lean angle. This is the angle of the steering wheel. Note that T_ϕ is not the torque applied to the handlebars as in the previous systems but the torque applied to bicycle in the roll direction of the bicycle. This method of input is illustrated in figure A.6(a) using a flowchart.

107

An analogy of this can be thought of as riding a bicycle without using your hands, letting go of the handlebars. Moving your body slowly to the left will impose a torque on the bicycle in the lean direction. Leaning right for example will make the bicycle make a right turn.

The value for K_{p2} was chosen experimentally. A large value of K_{p2} made the system unstable. A convenient value for K_{p2} turned out to be K_{p2}=40.

The result was a stable system, however not for all speeds. The rider is again unable to control the bicycle in the lower speed ranges.

Also when the bicycle has a roll angle to the right the natural response is to steer to the right in order to stabilize the bicycle. This effect is no longer present in this model. In this model steering to the left stabilizes the bicycle.

This input was incorporated in the final version of the program, the name of the corresponding file is **game_nohands.m**

A different attempt was done using the following changed input.

$$E = \phi_{desired} - \phi$$
$$T_\delta(t) = K_{p3} \cdot E \qquad \text{(A.12)}$$

Note that now not T_ϕ is used but T_δ, this means that this input is applied to the torque to the handlebars of the bicycle.
This method of input is illustrated in figure A.6(b) using a flowchart.

The value for K_{p3} is again chosen experimentally. An appropriate value was found to be K_{p3}=-4. The result was another stable system but still in the lower speed range the bicycle was uncontrollable. There was no improvement using this system.

Also when the bicycle has a roll angle to the right the natural response is to steer to the right in order to stabilize the bicycle. This effect is no longer present in this model. In this model steering to the left stabilizes the bicycle.

This input was incorporated in the final version of the program, the name of the corresponding file is **game_nolean.m**

Although now 3 working methods of input have been found none of these input provides a realistic method. For the following reasons.

- There is no counter steering effect

- The steer angle in the model is not equal to the steer angle of the steering wheel

- The rider is unable to stabilize the bicycle at a speed lower than 4.5 m/s
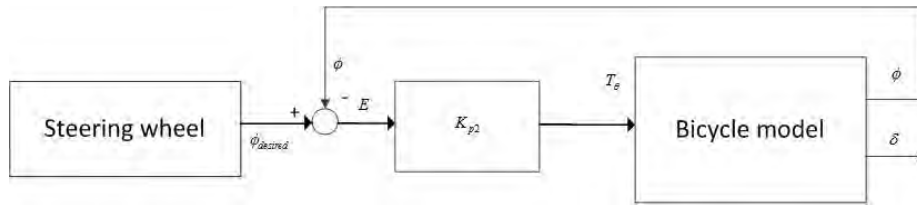
(a) A flowchart which shows how the Proportional controller for the simulator works. The block shown as "bicycle model" contains no more than equation 3.1
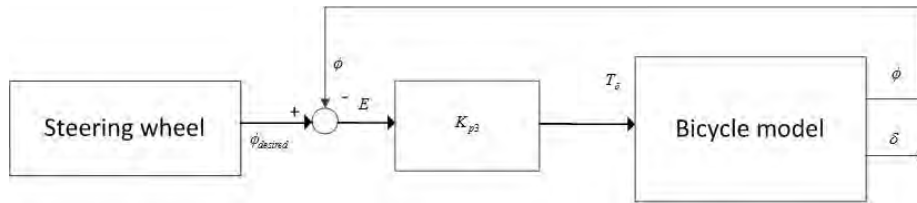
(b) A flowchart which shows how the Proportional controller for the simulator works. The block shown as "bicycle model" contains no more than equation 3.1

Figure A.6:

A method that could be able to achieve this is by using an LQR controller to regulate the torque applied to the model. However the amount of time that was available was not sufficient to be able to do this. For future development of this simulator , investigation of an LQR controller should be the first step.

As was mentioned earlier the dynamics of the system are changed by the methods of input that were shown in this section. The next section describes how the dynamics were changed.

A.4 Stability

Uncontrolled bicycle

The stability of the system can be calculated. The eigenfrequencies of the system are found through the characteristic equation A.13.

$$\left\{ M\lambda^2 + v\lambda + (K_0 g + v^2 K_2) \right\} q = 0 \tag{A.13}$$

The solutions of this equation are dependent of the speed v. They were shown previously in figure 8.1 and they are also shown in figure A.4.

For a more detailed explanation of the characteristic equation, the solutions and the meaning of these solution please see section 8.1.

In the figure can be seen that the stable speed range of he uncontrolled bicycle is [5 m/s to 7 m/s].

Controlled bicycle rotation based input of steer angle proportional controller

In section A.3 the following equation was used.

$$\begin{aligned} E &= \delta_{desired} - \delta \\ T_\delta &= K_{p1} \cdot E \end{aligned} \tag{A.9}$$

In order to calculate the stability of this system the equation is substituted in equation A.13. The result is the following equation.

$$M\ddot{q} + vC_1\dot{q} +_2 \left(K_0 g + v^2 K \right) q = \begin{bmatrix} 0 \\ K_{p1}(\delta_{desired} - \delta) \end{bmatrix} \tag{A.14}$$

The controlled bicycle has a different differential equation. Rewriting equation A.16 gives the following.

$$M\ddot{q} + vC_1\dot{q} + \left(K_0 g + v^2 K_2 + \begin{bmatrix} 0 & 0 \\ 0 & K_{p1} \end{bmatrix} \right) q = \begin{bmatrix} 0 \\ K_{p1}\delta_{desired} \end{bmatrix} \tag{A.15}$$

The characteristic equation for the homogeneous solution becomes the following.

$$M\ddot{q} + vC_1\dot{q} + \left(K_0 g + v^2 K_2 + \begin{bmatrix} 0 & 0 \\ 0 & K_{p1} \end{bmatrix} \right) q = 0 \tag{A.16}$$

The solutions of this equation with K_{p1}=-2 are dependent of the speed v. They are shown in figure A.4.

From the figure can be seen that the stable speed range has changed with respect to that of the uncontrolled bicycle. The stable speed range is now [5.5 m/s to 8 m/s].
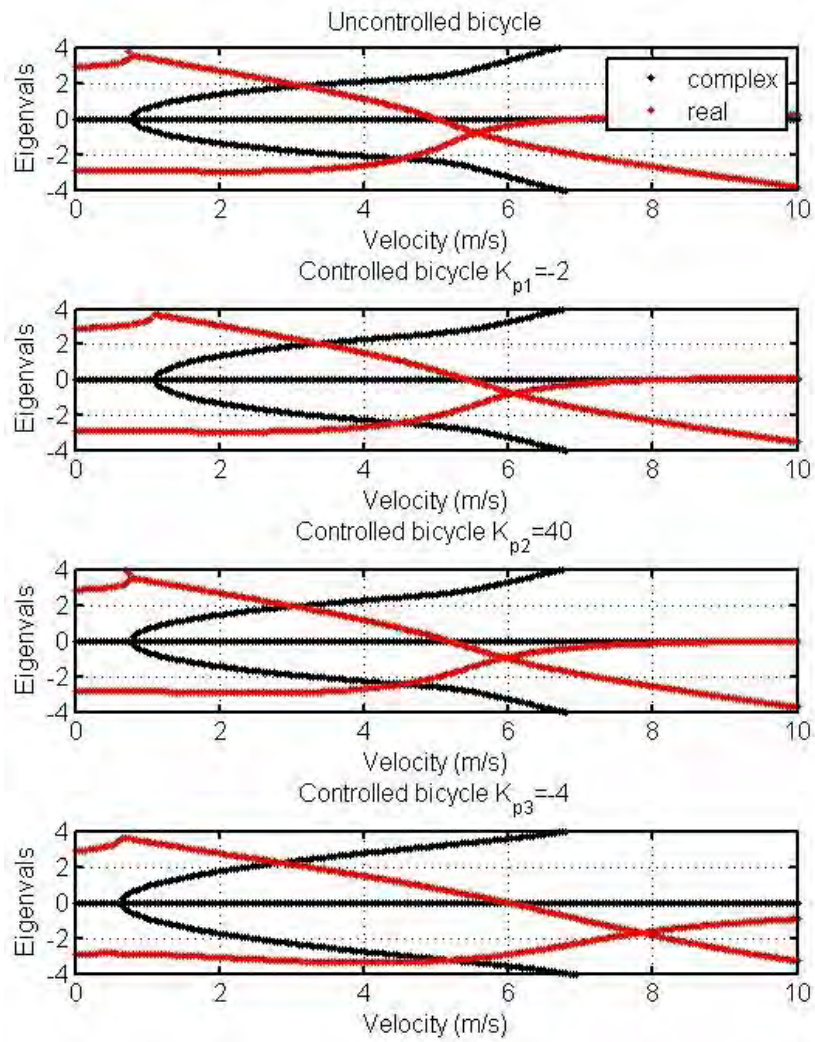
Figure A.7: The eigenvalues of the uncontrolled and controlled bicycle. The complex eigenvalues are shown in black.

Controlled bicycle rotation based input of lean angle proportional controller

In section A.3 the following equation was used to describe the proportional controller.

$$E = \phi_{desired} - \phi$$
$$T_\phi = K_{p2} \cdot E$$
(A.11)

When substituted into A.13, rewritten and converted to the homogeneous equation as done earlier in this section the following homogenous equation is found.

$$M\ddot{q} + vC_1\dot{q} + \left(K_0 g + v^2 K_2 + \begin{bmatrix} K_{p1} & 0 \\ 0 & 0 \end{bmatrix} \right) q = 0$$
(A.17)

The solutions of this equation with K_{p2}=40 are dependent of the speed v. They are shown in figure A.4.

In the figure can be seen that the stable speed range is now [5.3 m/s to 10 m/s].

In section A.3 also the following equation was used.

$$E = \phi_{desired} - \phi$$
$$T_\delta(t) = K_{p3} \cdot E$$
(A.12)

The stability of this system is found in a similar manner as was done earlier in this section. The homogeneous equation becomes the following.

$$M\ddot{q} + vC_1\dot{q} + \left(K_0 g + v^2 K_2 + \begin{bmatrix} 0 & 0 \\ K_{p3} & 0 \end{bmatrix} \right) q = 0$$
(A.18)

The solutions of this equation with K_{p3}=-4 are dependent of the speed v. They are shown in figure A.4.

In the figure can be seen that the start of the stable speed range is now at 6 m/s the end of the stable speed range is not visible in the figure. The range ends beyond 30 m/s.

Bibliography

[1] J. P. Meijaard, Jim M. Papadopoulos, Andy Ruina, A. L. Schwab, "Linearized dynamics equations for the balance and steer of a bicycle: a benchmark and review", Proceedings of the Royal Society A 463:1955-1982. **(2007)**

[2] J. K. Moore, M. Hubbard, J. D. G. Kooijman and A. L. Schwab, "A method for estimating physical properties of a combined bicycle and rider," In Proceedings of the ASME 2009 International Design Engineering Technical Conferences and Computers and Information in Engineering Conference, DETC2009, Aug 30 - Sep 2, 2009, San Diego, CA. **2009**

[3] A. L. Schwab and J. D. G. Kooijman, Lateral dynamics of a bicycle with passive rider model **2010**

[4] Wilson, D. G., Bicycling Science, ISBN: 0-262-73154-1 **1928**

[5] F.M. Dekking, C. Kraaikamp, H.P. Lopuha, L.E. Meester, A Modern Introduction to Probability and Statistics, ISBN: 1852338962 **2005**

[6] V. Cossalter, R. Lot, S. Rota, "On the Validation of a Motorcycle Riding Simulator" **2010**

[7] V. Cossalter, R. Lot, S. Rota, Objective and subjective evaluation of an advanced motorcycle riding simulator **2010**

[8] F.J.W. Whipple, The stability of the motion of a bicycle. The Quarterly Journal of Pure and Applied Mathematics Vol. 30 pp.312-348 **1899**

[9] Kok Y. Cheng, David Bothman, Karl J. strm, Bicycle Torque Sensor Experiment **2003**

[10] Stichting Wetenschappelijk Onderzoek Verkeersveiligheid. Factsheet, Ouderen in het verkeer **2008**

[11] S. M. Cain and N. C. Perkins. Comparison of a Bicycle Steady-State Turning Model to Experimental Data **2010**